

Supporting Information

Distinctive Nucleic Acid Recognition by Lysine-Embedded Phenanthridine Peptides

Josipa Matic¹, Patrycysz Piotrowski², Lucija Vrban³, Renata Kobetic¹, Robert Vianello³, Ivona Jurić¹, Ivana Fabijanić¹, Margareta Pernar Kovač⁴, Anamaria Brozovic⁴, Ivo Piantanida¹, Carsten Schmuck^{2,†} and Marijana Radić Stojković^{1,*}

¹ Laboratory for Biomolecular Interactions and Spectroscopy, Division of Organic Chemistry and Biochemistry, Ruđer Bošković Institute, Bijenička cesta 54, 10000 Zagreb, Croatia;

josipa.matic@gmail.com (J.M.); renata.kobetic@irb.hr (R.K.); juric.ivona@student.pmf.hr (I.J.);

i.s.fabijanic@gmail.com (I.F.); ivo.piantanida@irb.hr (I.P.)

² Institute for Organic Chemistry, University of Duisburg-Essen, Universitätsstrasse 7, 45141 Essen, Germany; p.piotrowski@gmx.net (P.P.); carsten.schmuck@uni-due.de (C.S.)

³ Laboratory for the Computational Design and Synthesis of Functional Materials, Division of Organic Chemistry and Biochemistry, Ruđer Bošković Institute, Bijenička cesta 54, 10000 Zagreb, Croatia; lvrban@irb.hr (L.V.); robert.vianello@irb.hr (R.V.)

⁴ Division of Molecular Biology, Ruđer Bošković Institute, Bijenička cesta 54, 10000 Zagreb, Croatia; margareta.pernar@irb.hr (M.P.K.); anamaria.brozovic@irb.hr (A.B.)

* Correspondence: mradic@irb.hr; Tel.: +385-1-4571220; Fax: +385-1-4680195

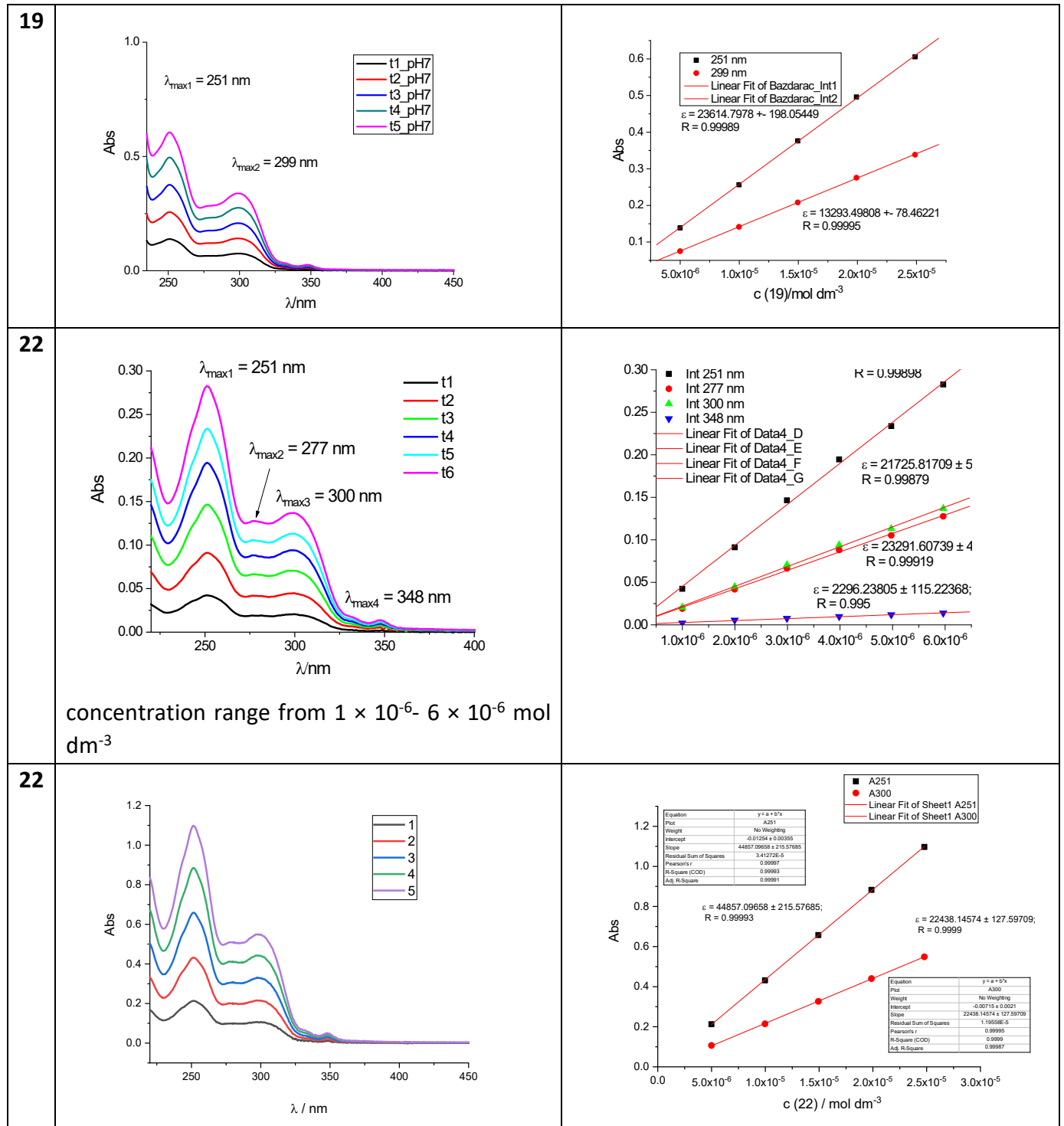
† Deceased 1 August 2019.

Contents

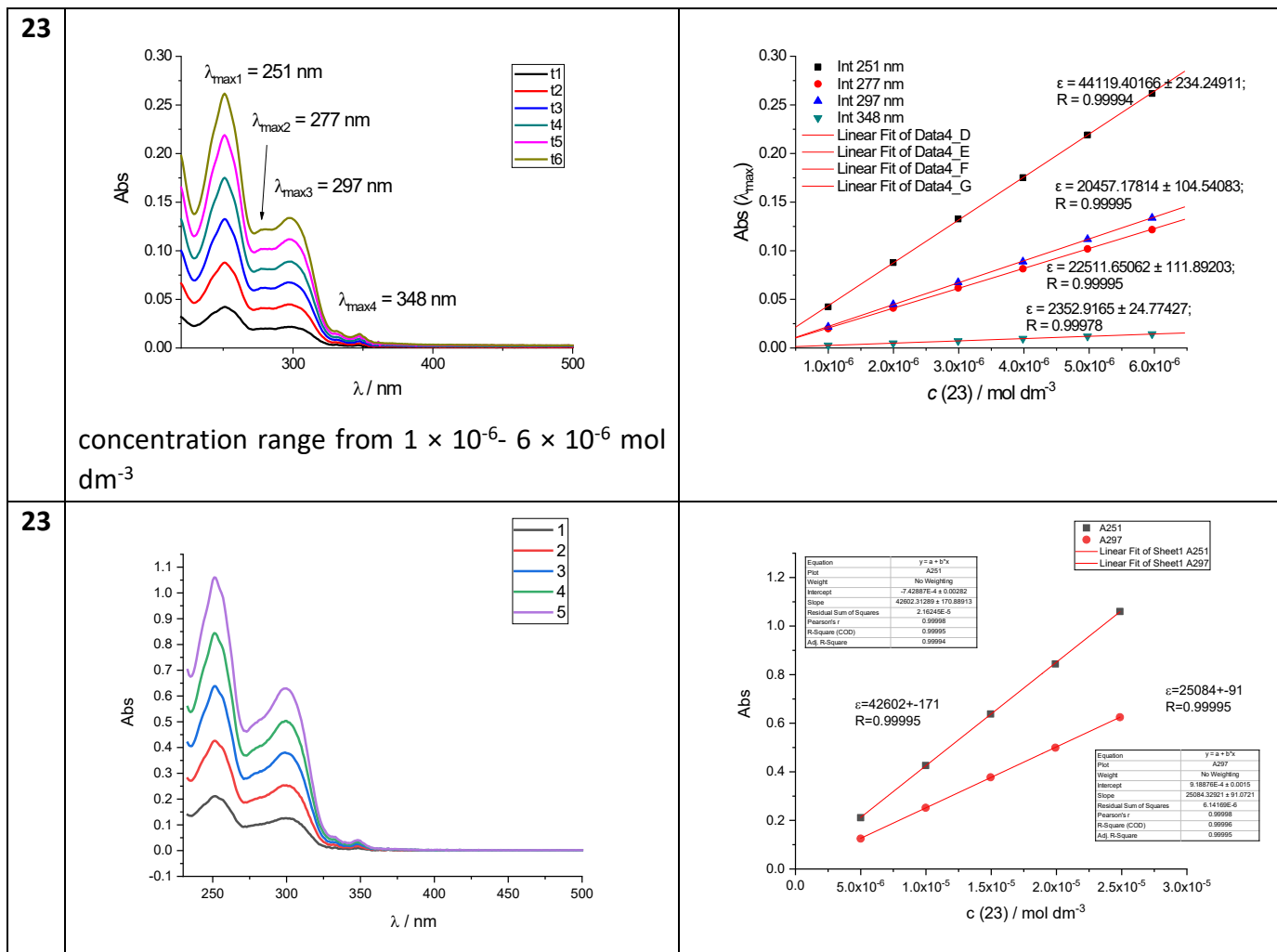
1. Spectroscopic characterization of phenanthridine peptides in aqueous solutions.
2. Interactions of phenanthridine peptides with polynucleotides in neutral and weakly acid medium (pH 7.0 and pH 5.0)
 - 2.1. Fluorimetric titrations
 - 2.2. Thermal melting experiments
 - 2.3. Circular dichroism (CD) titrations
 - 2.4. Mass spectra
3. Computational analysis of **19**, **22** and **23**

1. Spectroscopic characterization of phenanthridine peptides in aqueous solutions

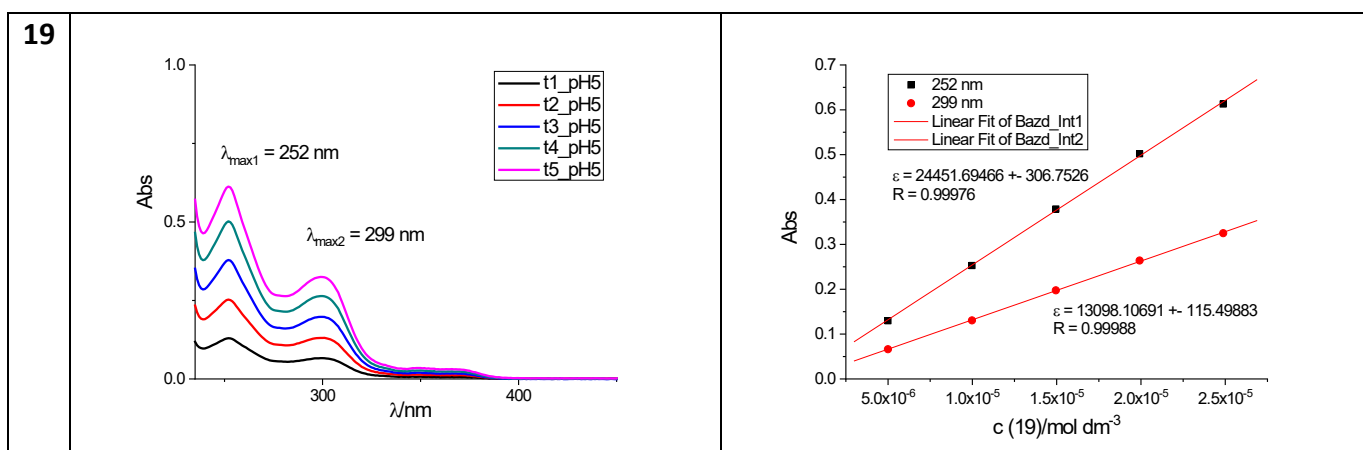
1.1. UV/Vis spectra at pH 7.0



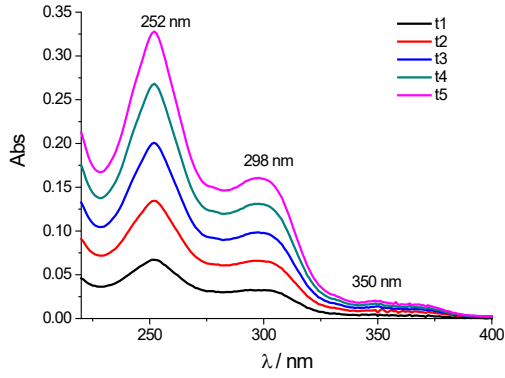
concentration range from 1×10^{-6} - 6×10^{-6} mol dm^{-3}



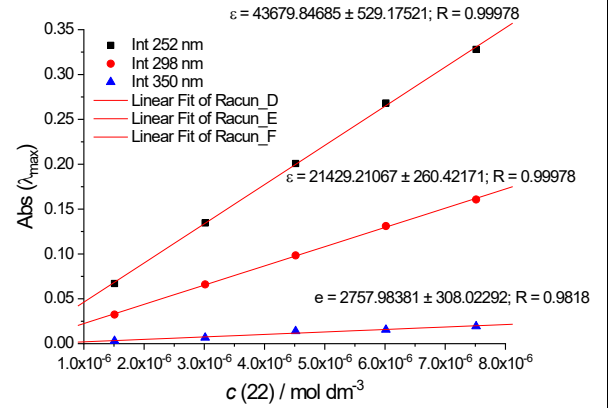
1.2. UV/Vis spectra at pH 5.0



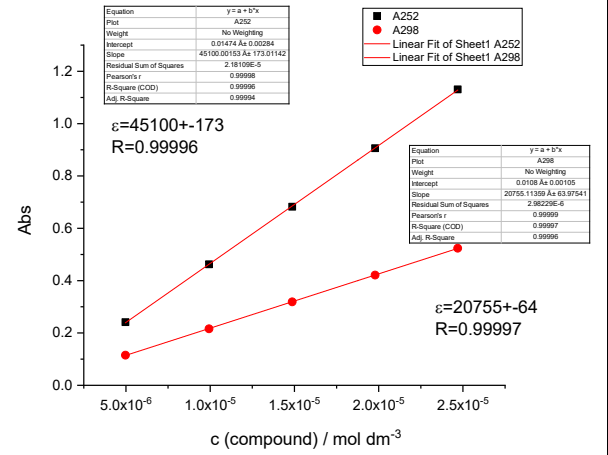
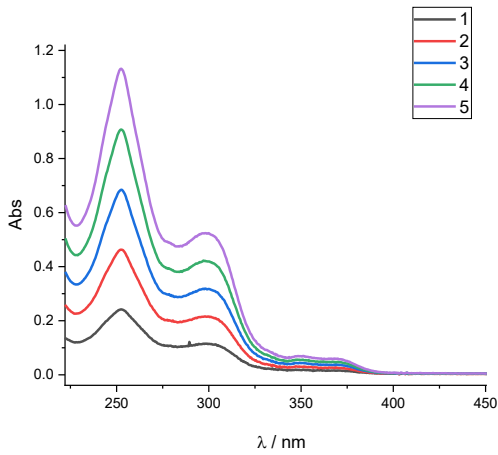
22



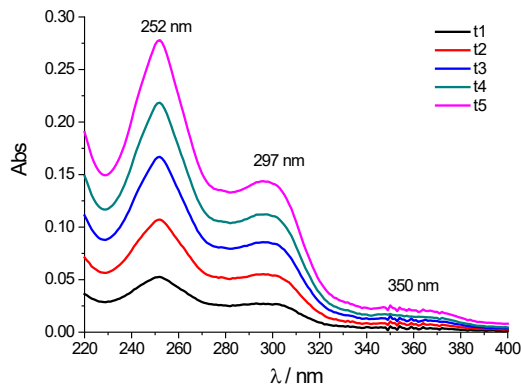
concentration range from 1×10^{-6} - 6×10^{-6} mol dm^{-3}



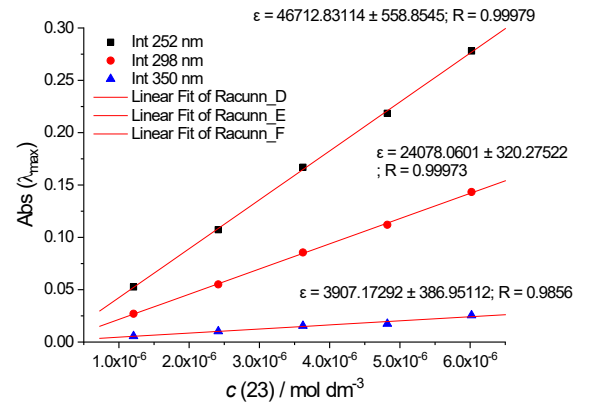
22



23



concentration range from 1×10^{-6} - 6×10^{-6} mol dm^{-3}



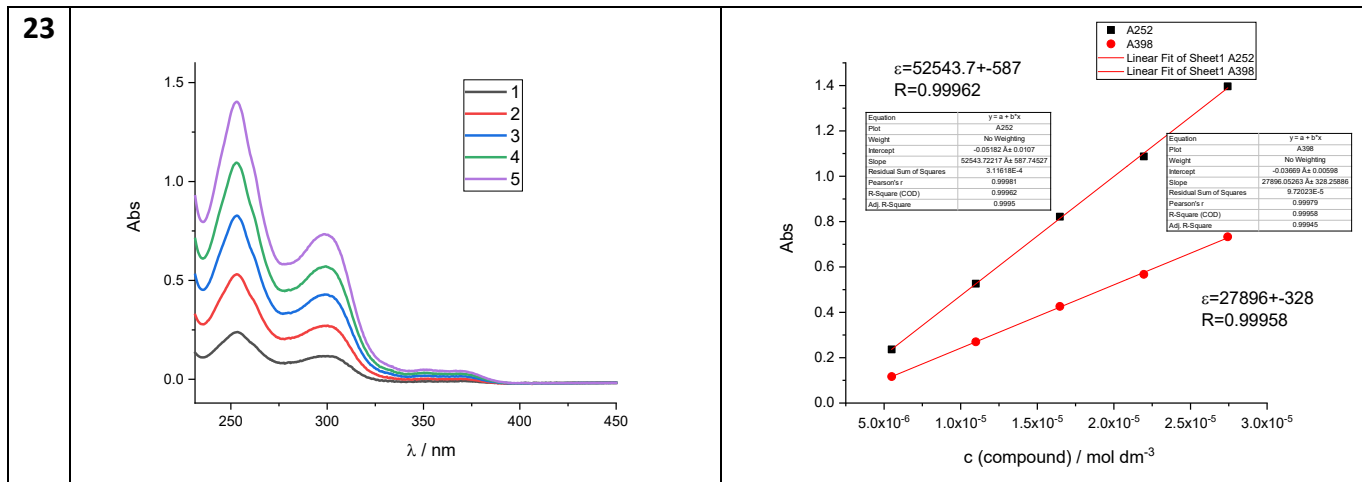
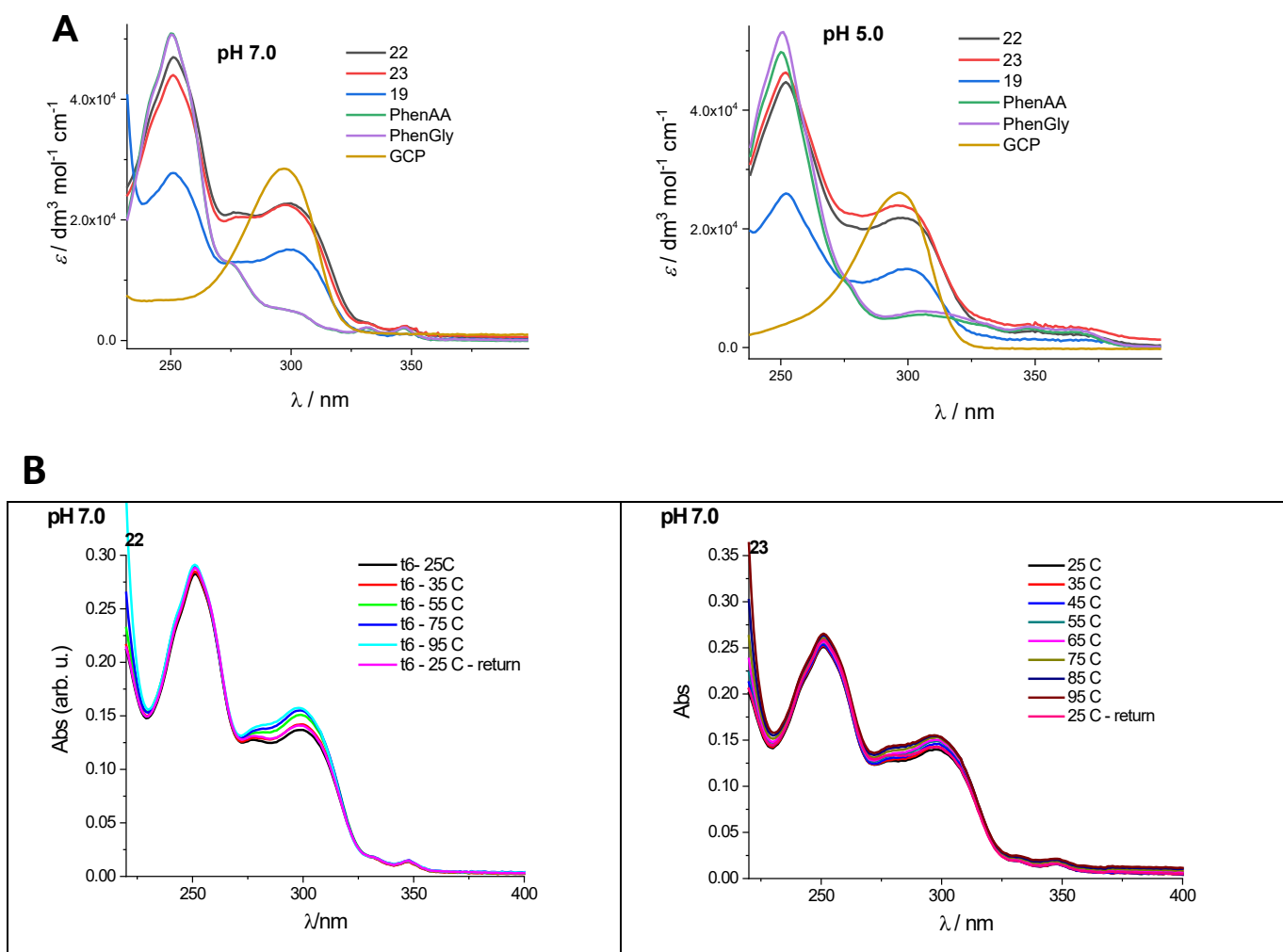


Figure S2. UV/Vis spectra changes of **19,22,23** at different concentrations (concentration range from 5×10^{-6} - 2.5×10^{-5} mol dm⁻³) at pH 5.0, sodium cacodylate buffer, $I=0,05$ M.



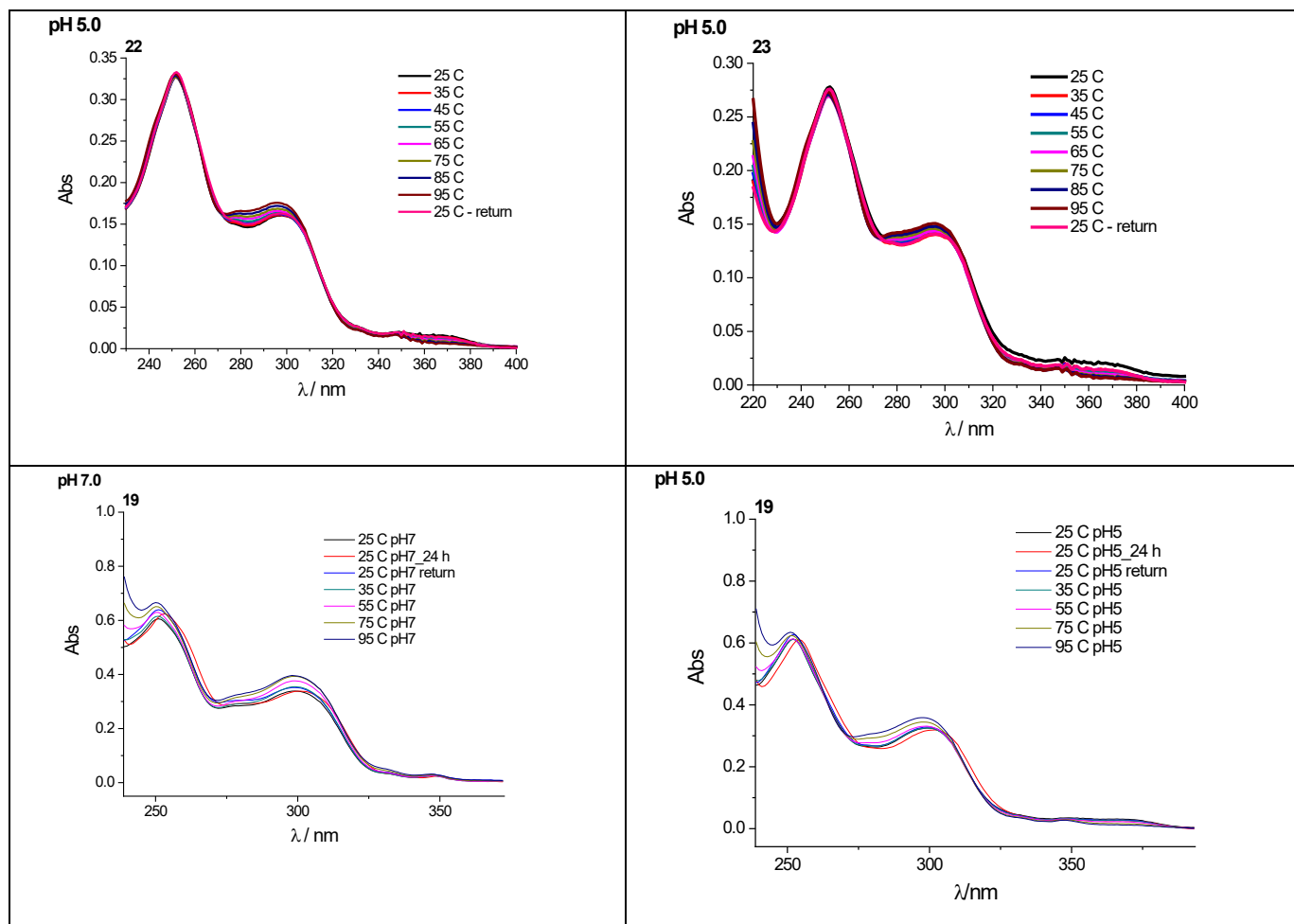
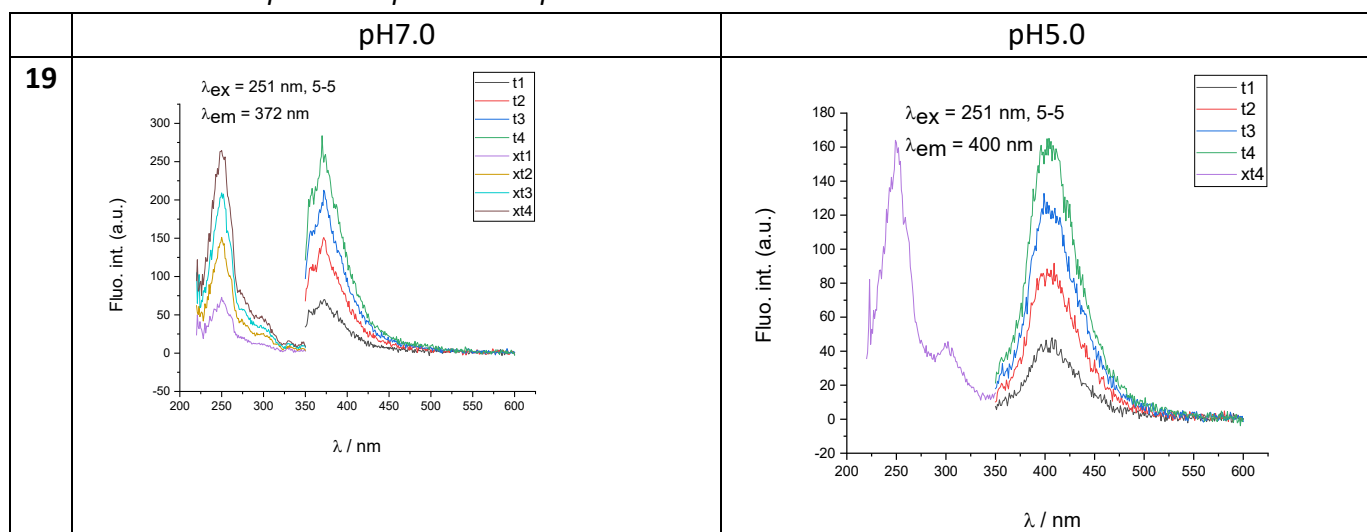


Figure S3. A) Overlapped UV spectra of **22**, **23** and **19** with the reference compounds **Phen-AA**, **Phen-Gly** and **GCP**; showing hypochromicity of all chromophores; B) changes of UV spectra of **22**, **23** and **19** upon temperature increase.

1.3. Fluorescence spectra at pH 7.0 and pH 5.0



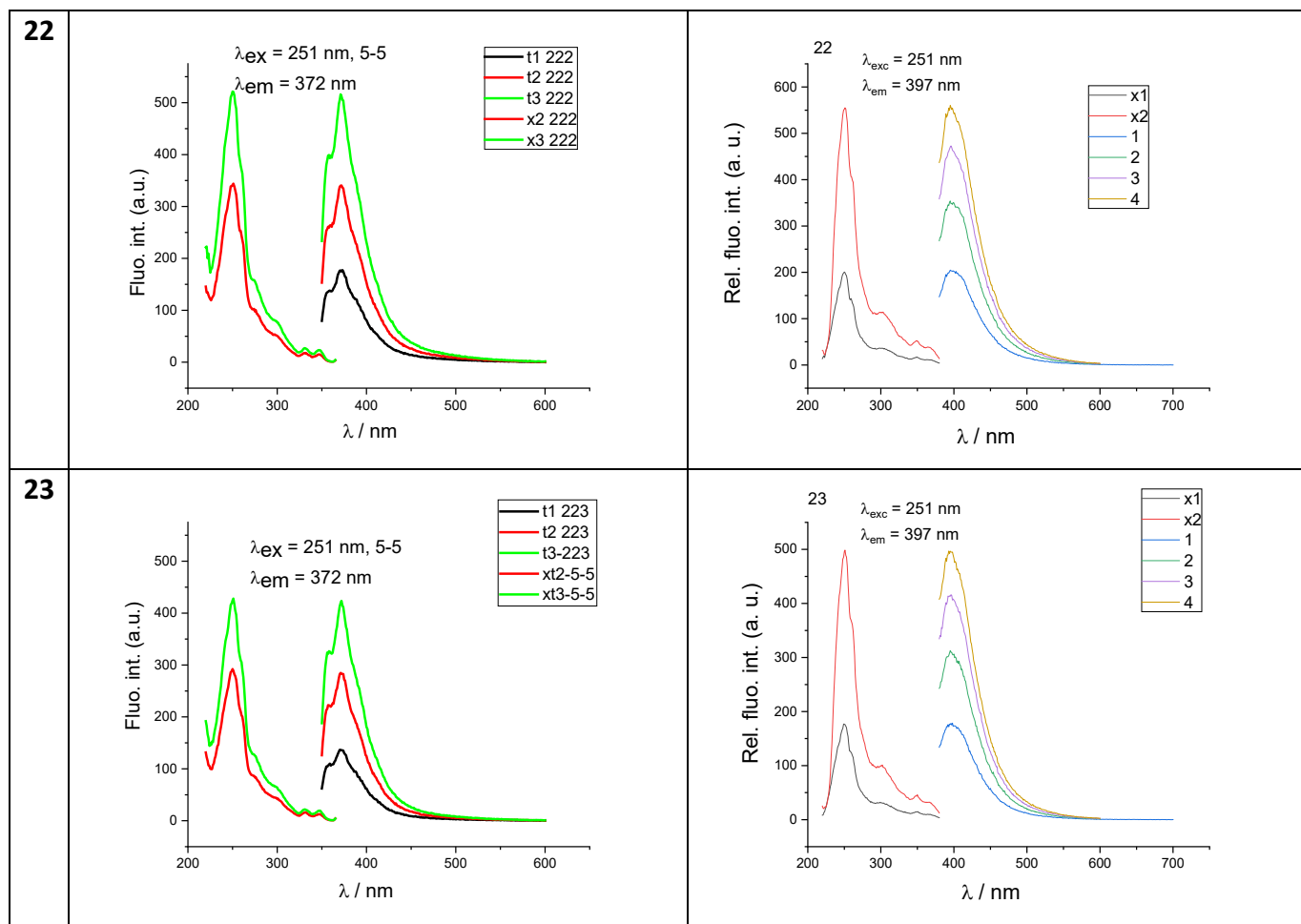
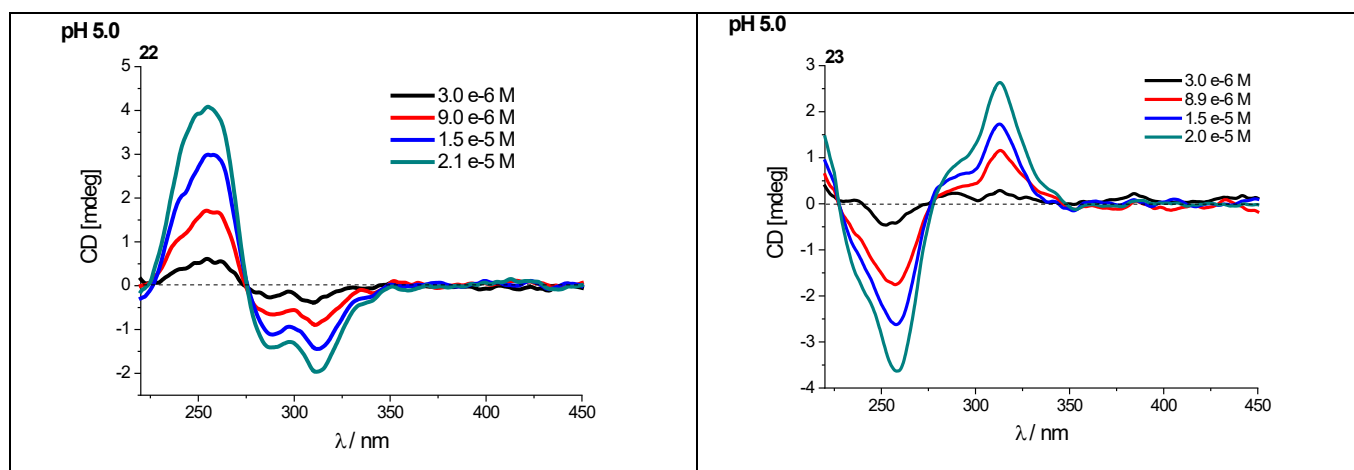


Figure S4. Emission and excitation spectra changes of **19**, **22**, **23** at different concentrations at $\lambda_{exc}=251$ nm (concentration range from 5×10^{-7} - 2×10^{-6} mol dm⁻³) at pH 7.0 and pH 5.0, Na cacodylate buffer, $I=0.05$ mol dm⁻³.

1.4. CD spectra of **19**, **22** and **23**



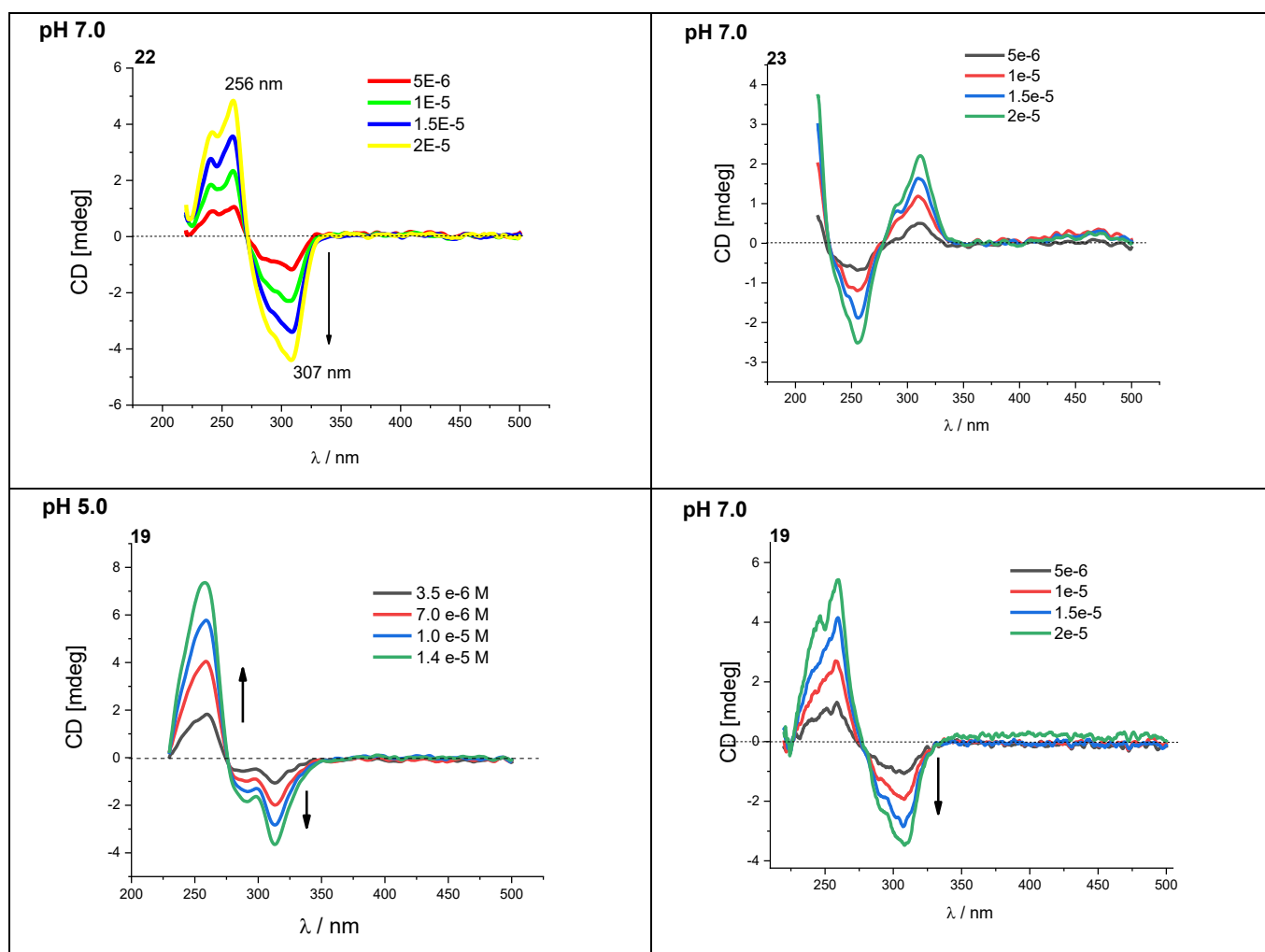


Figure S5. CD spectra changes of **19**, **22** and **23** at different concentrations (concentration range from 3.0×10^{-6} - 6×10^{-5} mol dm⁻³) at pH = 7.0 and 5.0 (buffer sodium cacodylate, $I = 0.05$ mol dm⁻³).

2. Interactions of phenanthridine peptides with polynucleotides in neutral and weakly acid medium (pH 7.0 and pH 5.0)

2.1. Fluorimetric titrations

2.1.1. Fluorimetric titrations at pH 7.0

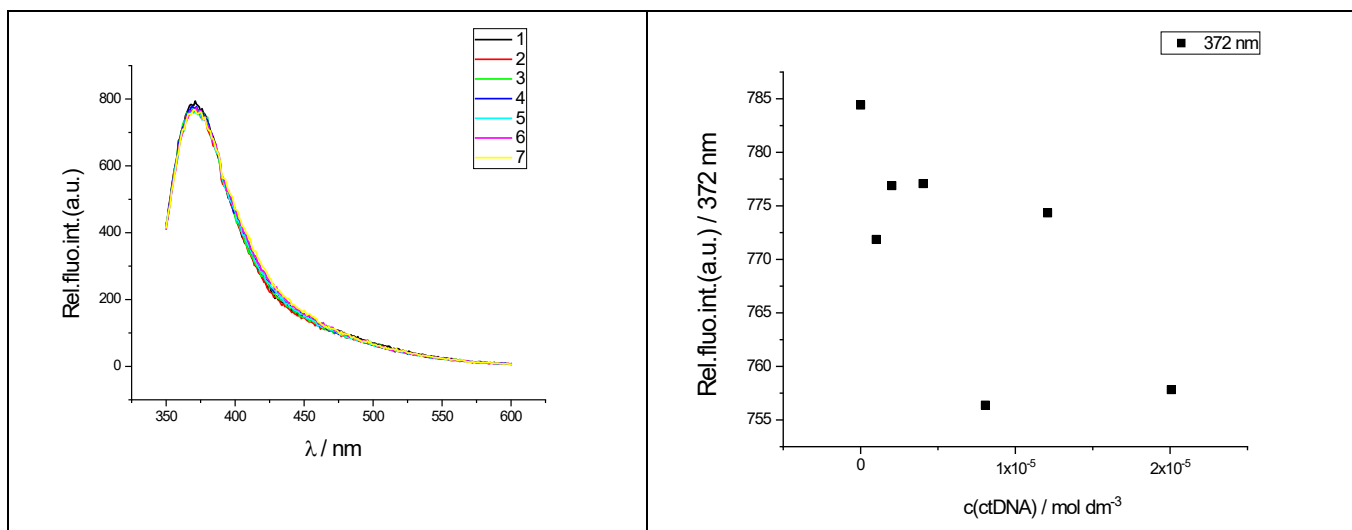


Figure S6. a) Changes in fluorescence spectrum of **19** ($c = 1.0 \times 10^{-6} \text{ mol dm}^{-3}$, $\lambda_{\text{exc}} = 300 \text{ nm}$) upon titration with ctDNA ($c = 1.0 \times 10^{-6} - 2 \times 10^{-5} \text{ mol dm}^{-3}$); b) Dependence of **19** absorbance at $\lambda_{\text{max}} = 372 \text{ nm}$ on $c(\text{ctDNA})$, at pH 7.0, sodium cacodylate buffer, $I = 0.05 \text{ mol dm}^{-3}$.

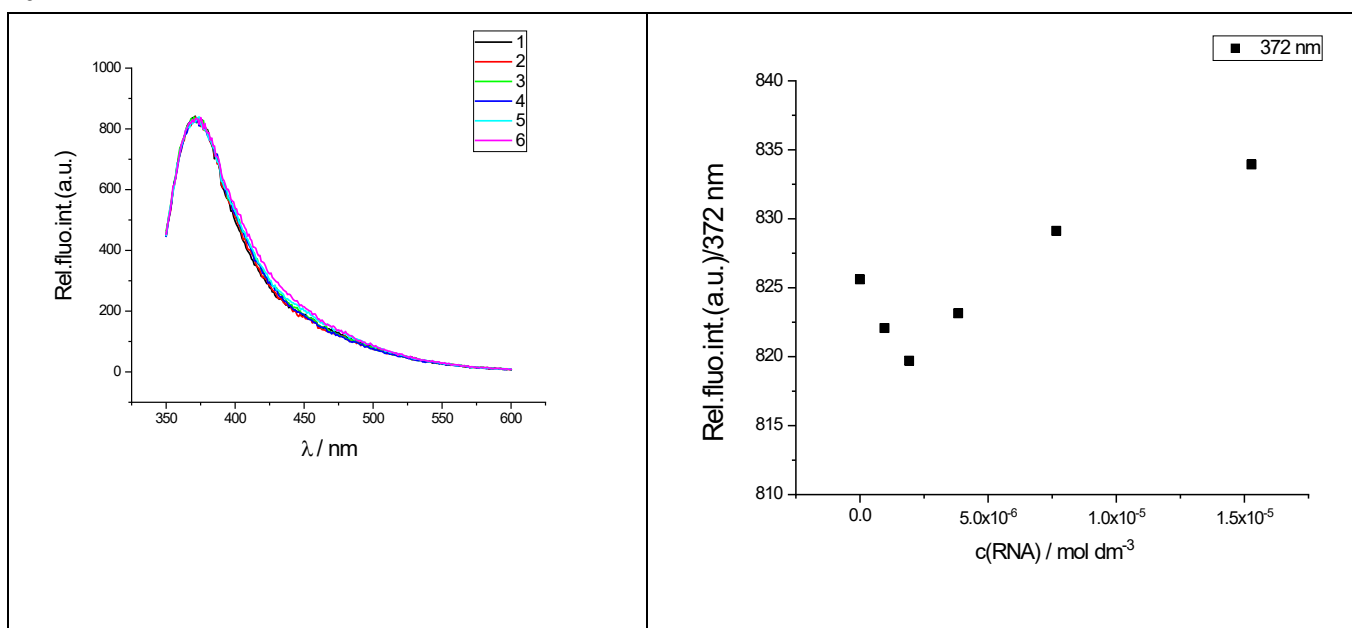


Figure S7. a) Changes in fluorescence spectrum of **19** ($c = 1.0 \times 10^{-6} \text{ mol dm}^{-3}$, $\lambda_{\text{exc}} = 300 \text{ nm}$) upon titration with poly A-poly U ($c = 1.0 \times 10^{-6} - 1.9 \times 10^{-5} \text{ mol dm}^{-3}$); b) Dependence of **19** absorbance at $\lambda_{\text{max}} = 372 \text{ nm}$ on $c(\text{poly A-poly U})$, at pH 7.0, sodium cacodylate buffer, $I = 0.05 \text{ mol dm}^{-3}$.

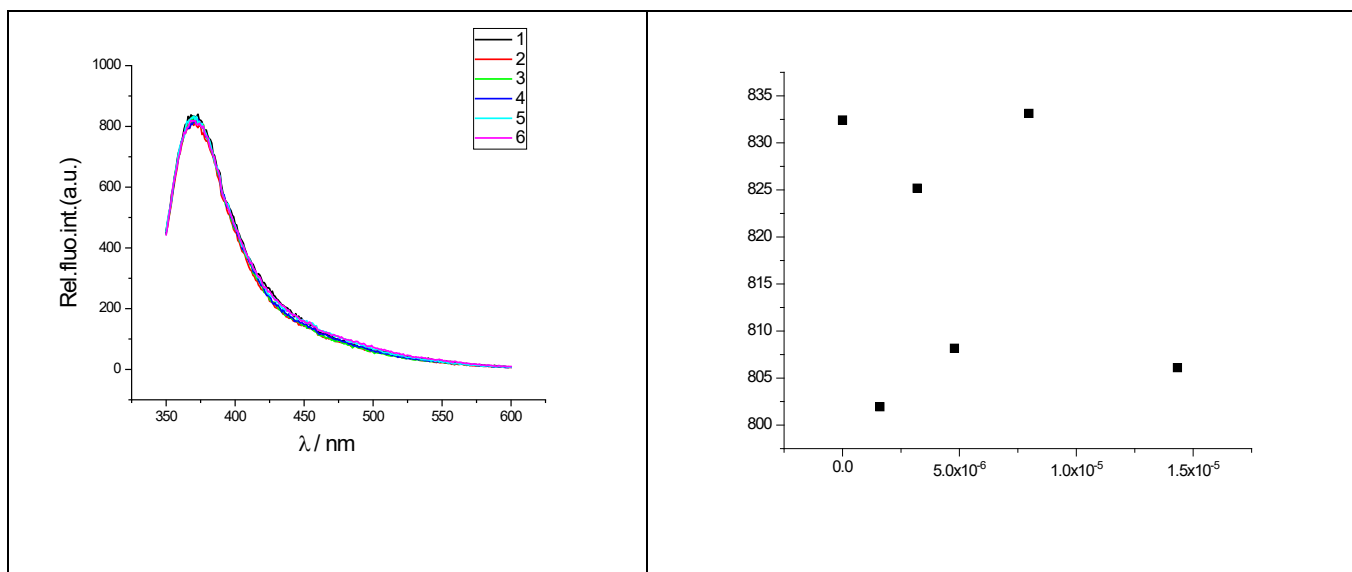


Figure S8. a) Changes in fluorescence spectrum of **19** ($c = 1.0 \times 10^{-6} \text{ mol dm}^{-3}$, $\lambda_{\text{exc}} = 300 \text{ nm}$) upon titration with poly(dGdC)₂ ($c = 1.6 \times 10^{-6} - 1.4 \times 10^{-5} \text{ mol dm}^{-3}$); b) Dependence of **19** absorbance at $\lambda_{\text{max}} = 372 \text{ nm}$ on $c(\text{poly}(\text{dGdC})_2)$, at pH 7.0, sodium cacodylate buffer, $I = 0.05 \text{ mol dm}^{-3}$.

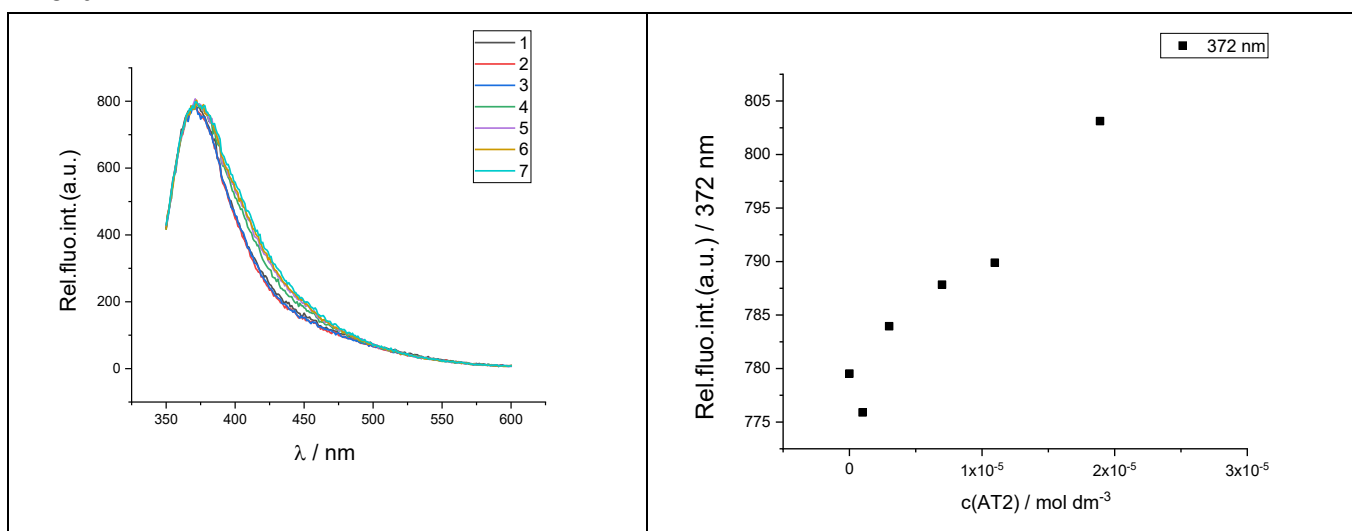


Figure S9. a) Changes in fluorescence spectrum of **19** ($c = 1.0 \times 10^{-6} \text{ mol dm}^{-3}$, $\lambda_{\text{exc}} = 300 \text{ nm}$) upon titration with poly(dAdT)₂ ($c = 1.0 \times 10^{-6} - 1.9 \times 10^{-5} \text{ mol dm}^{-3}$); b) Dependence of **19** absorbance at $\lambda_{\text{max}} = 372 \text{ nm}$ on $c(\text{poly}(\text{dAdT})_2)$, at pH 7.0, sodium cacodylate buffer, $I = 0.05 \text{ mol dm}^{-3}$.

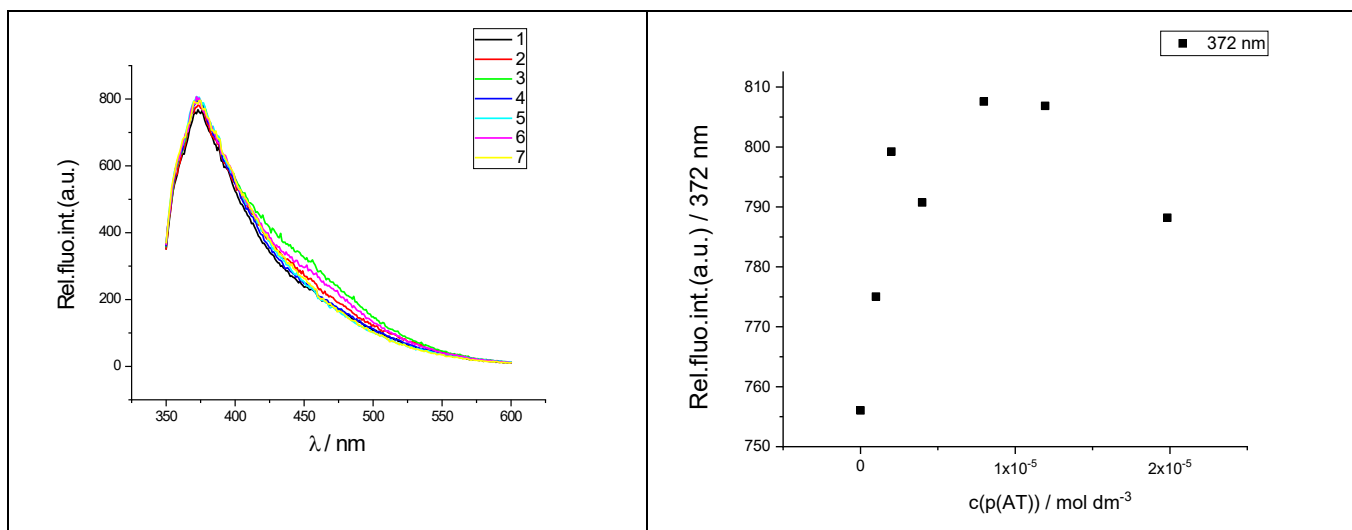


Figure S10. a) Changes in fluorescence spectrum of **19** ($c = 1.0 \times 10^{-6} \text{ mol dm}^{-3}$, $\lambda_{\text{exc}} = 300 \text{ nm}$) upon titration with poly dA-poly dT ($c = 1.0 \times 10^{-6} - 2.0 \times 10^{-5} \text{ mol dm}^{-3}$); b) Dependence of **19** absorbance at $\lambda_{\text{max}} = 372 \text{ nm}$ on $c(\text{poly dA-poly dT})$, at pH 7.0, sodium cacodylate buffer, $I = 0.05 \text{ mol dm}^{-3}$.

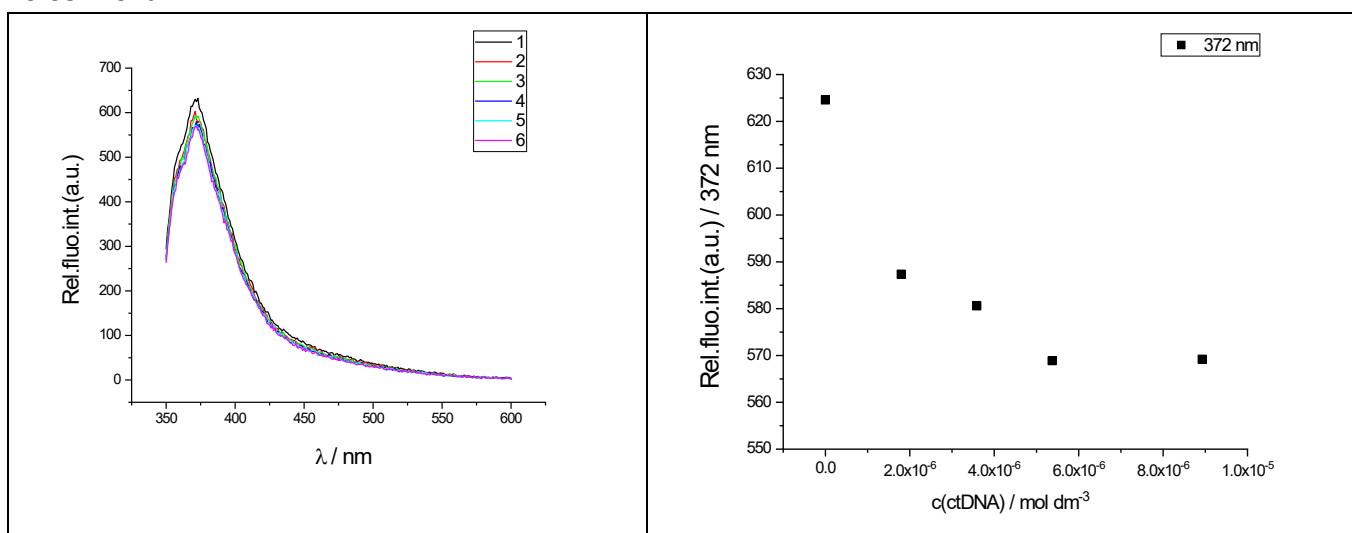


Figure S11. a) Changes in fluorescence spectrum of **22** ($c = 1.0 \times 10^{-6} \text{ mol dm}^{-3}$, $\lambda_{\text{exc}} = 300 \text{ nm}$) upon titration with ctDNA ($c = 9.0 \times 10^{-7} - 9 \times 10^{-6} \text{ mol dm}^{-3}$); b) Dependence of **22** absorbance at $\lambda_{\text{max}} = 372 \text{ nm}$ on $c(\text{ctDNA})$, at pH 7.0, sodium cacodylate buffer, $I = 0.05 \text{ mol dm}^{-3}$.

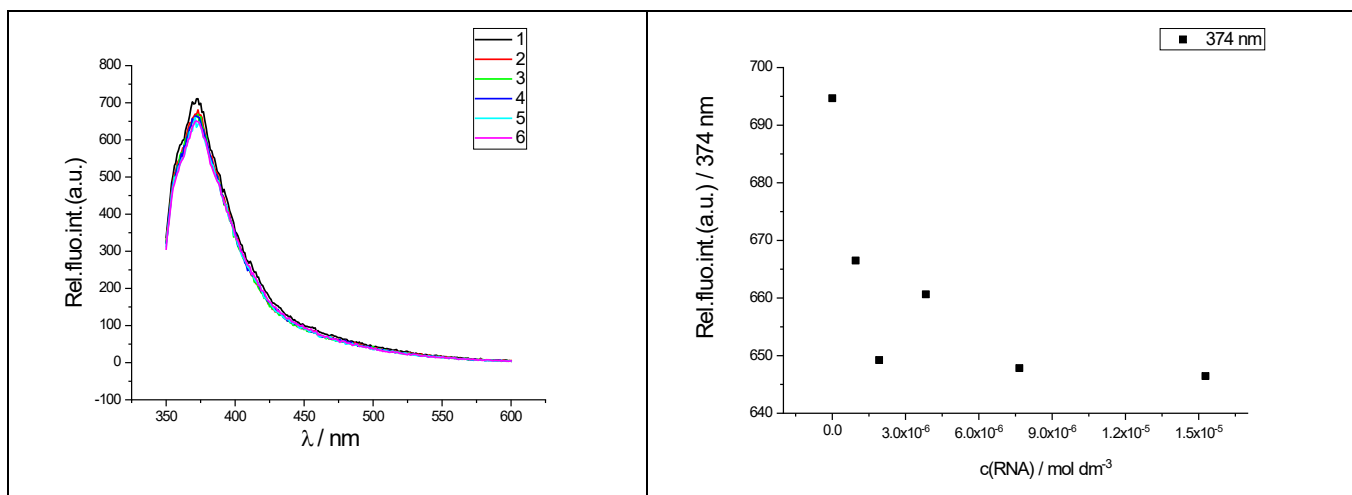


Figure S12. a) Changes in fluorescence spectrum of **22** ($c = 1.0 \times 10^{-6} \text{ mol dm}^{-3}$, $\lambda_{\text{exc}} = 300 \text{ nm}$) upon titration with poly A-poly U ($c = 1.0 \times 10^{-6} - 1.5 \times 10^{-5} \text{ mol dm}^{-3}$); b) Dependence of **22** absorbance at $\lambda_{\text{max}} = 374 \text{ nm}$ on $c(\text{poly A-poly U})$, at pH 7.0, sodium cacodylate buffer, $I = 0.05 \text{ mol dm}^{-3}$.

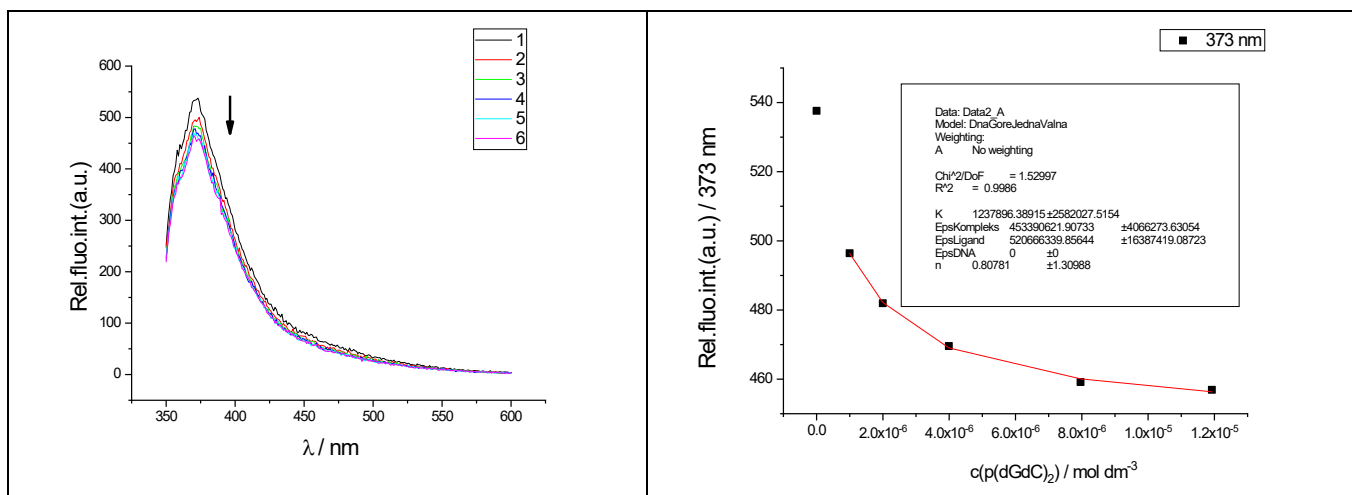


Figure S13. a) Changes in fluorescence spectrum of **22** ($c = 1.0 \times 10^{-6} \text{ mol dm}^{-3}$, $\lambda_{\text{exc}} = 300 \text{ nm}$) upon titration with poly(dGdC)₂ ($c = 1.0 \times 10^{-6} - 1.2 \times 10^{-5} \text{ mol dm}^{-3}$); b) Dependence of **22** absorbance at $\lambda_{\text{max}} = 373 \text{ nm}$ on $c(\text{poly(dGdC)}_2)$, at pH 7.0, sodium cacodylate buffer, $I = 0.05 \text{ mol dm}^{-3}$.

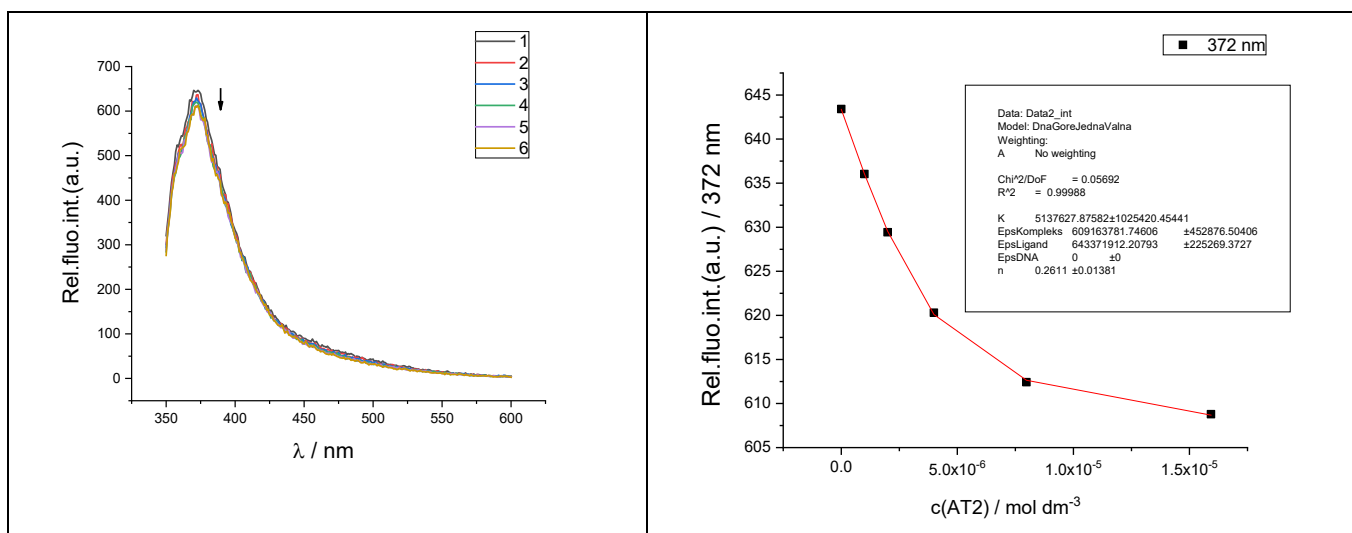


Figure S14. a) Changes in fluorescence spectrum of **22** ($c = 1.0 \times 10^{-6} \text{ mol dm}^{-3}$, $\lambda_{\text{exc}} = 300 \text{ nm}$) upon titration with poly(dAdT)₂ ($c = 1.0 \times 10^{-6} - 1.6 \times 10^{-5} \text{ mol dm}^{-3}$); b) Dependence of **22** absorbance at $\lambda_{\text{max}} = 372 \text{ nm}$ on $c(\text{poly(dAdT)}_2)$, at pH 7.0, sodium cacodylate buffer, $I = 0.05 \text{ mol dm}^{-3}$.

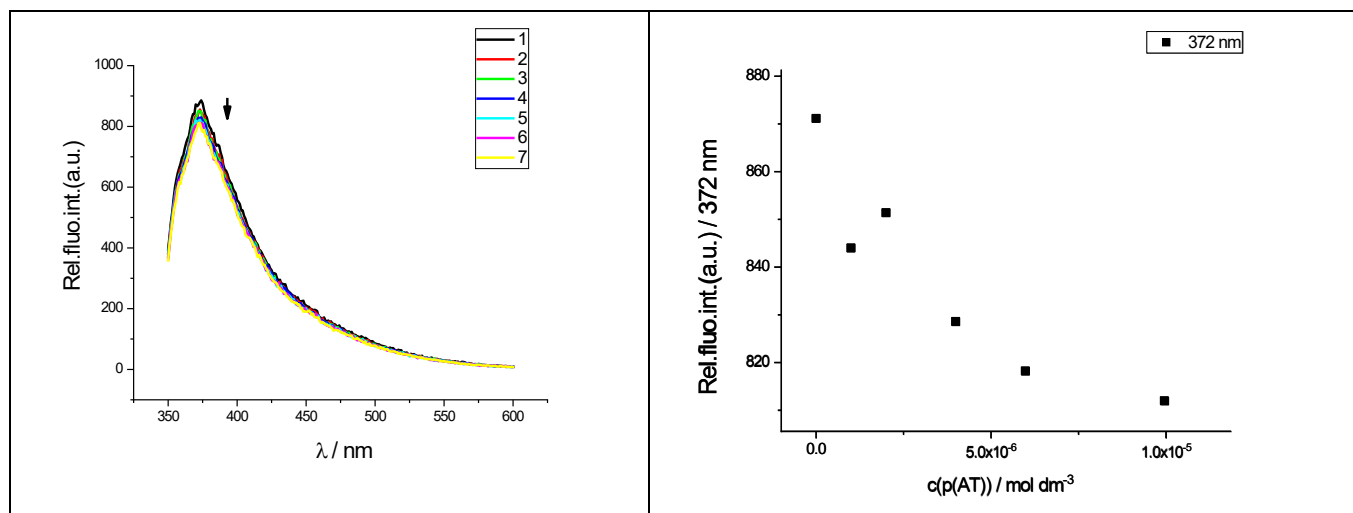


Figure S15. a) Changes in fluorescence spectrum of **22** ($c = 1.0 \times 10^{-6} \text{ mol dm}^{-3}$, $\lambda_{\text{exc}} = 300 \text{ nm}$) upon titration with poly dA-poly dT ($c = 1.0 \times 10^{-6} - 1.8 \times 10^{-5} \text{ mol dm}^{-3}$); b) Dependence of **22** absorbance at $\lambda_{\text{max}} = 372 \text{ nm}$ on $c(\text{poly dA-poly dT})$, at pH 7.0, sodium cacodylate buffer, $I = 0.05 \text{ mol dm}^{-3}$.

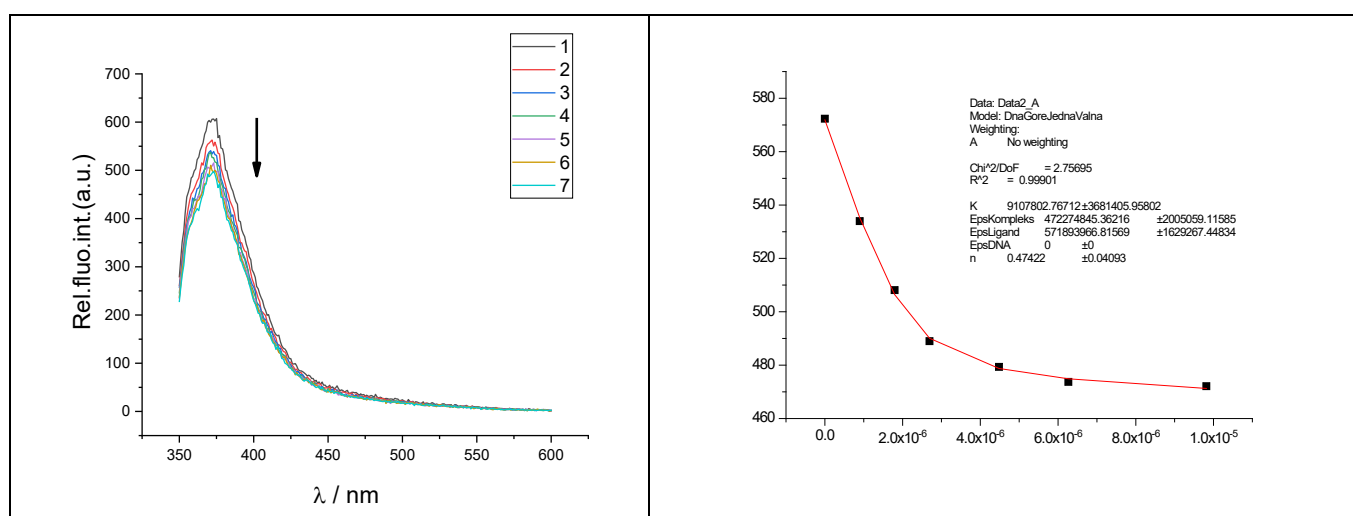


Figure S16. a) Changes in fluorescence spectrum of **23** ($c = 1.0 \times 10^{-6} \text{ mol dm}^{-3}$, $\lambda_{\text{exc}} = 300 \text{ nm}$) upon titration with ctDNA ($c = 1.0 \times 10^{-6} - 9.82 \times 10^{-6} \text{ mol dm}^{-3}$); b) Dependence of **23** absorbance at $\lambda_{\text{max}} = 377 \text{ nm}$ on $c(\text{ctDNA})$, at pH 7.0, sodium cacodylate buffer, $I = 0.05 \text{ mol dm}^{-3}$.

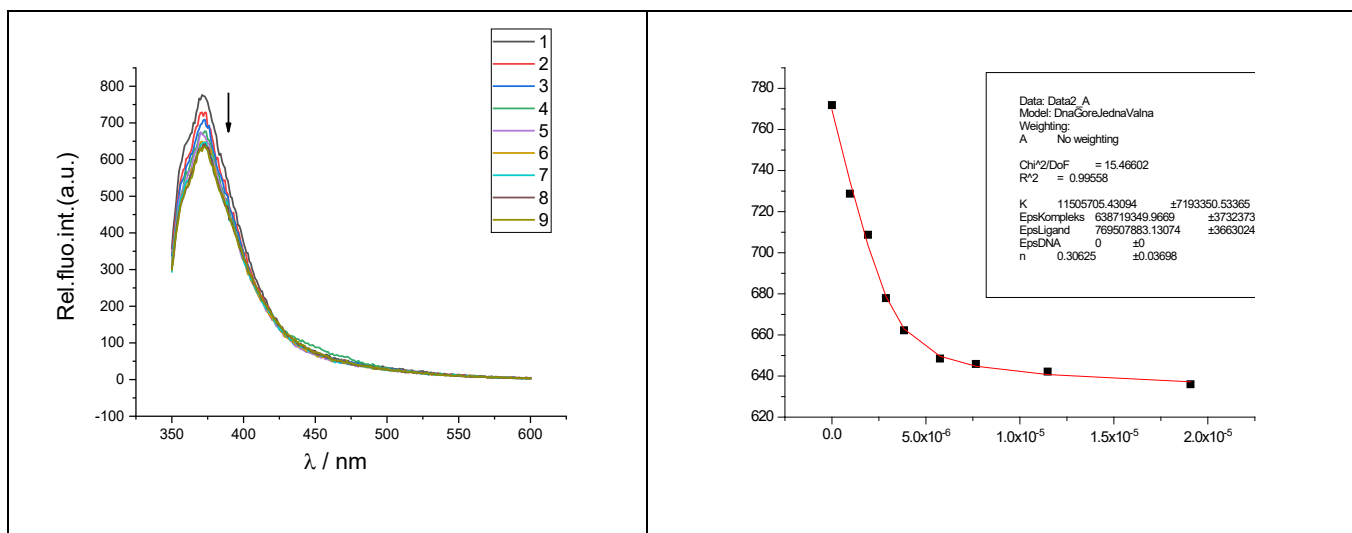


Figure S17. a) Changes in fluorescence spectrum of **23** ($c = 1.0 \times 10^{-6} \text{ mol dm}^{-3}$, $\lambda_{\text{exc}}=300 \text{ nm}$) upon titration with poly A-poly U ($c = 1.0 \times 10^{-6} - 1.9 \times 10^{-5} \text{ mol dm}^{-3}$); b) Dependence of **23** absorbance at $\lambda_{\text{max}} = 373 \text{ nm}$ on $c(\text{poly A-poly U})$, at pH 7.0, sodium cacodylate buffer, $I = 0.05 \text{ mol dm}^{-3}$.

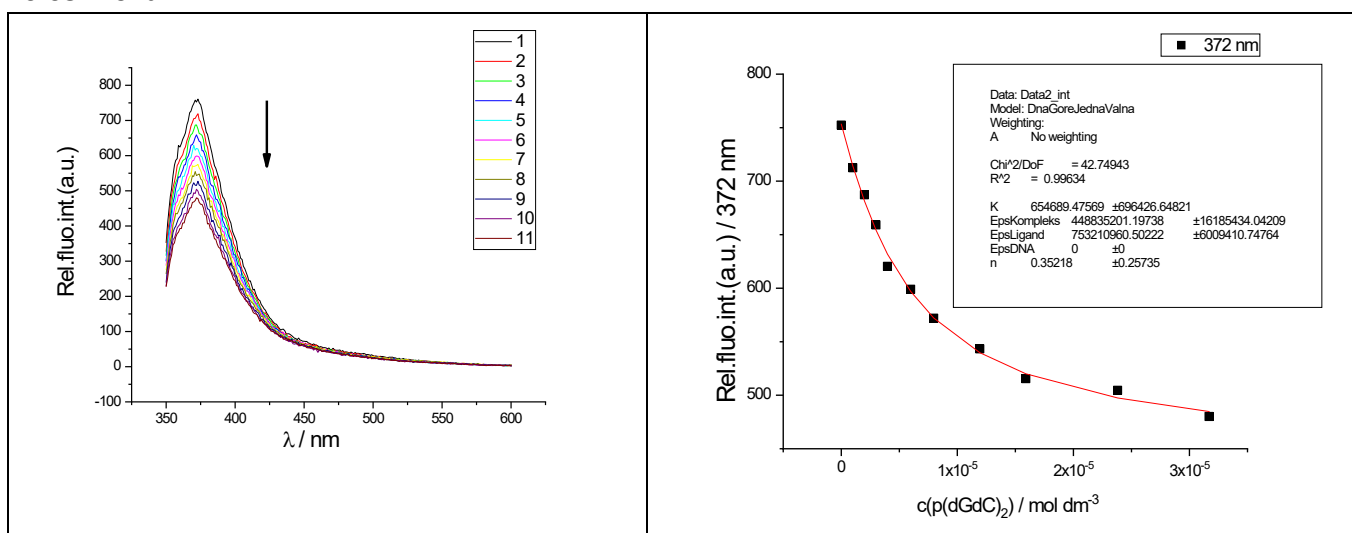


Figure S18. a) Changes in fluorescence spectrum of **23** ($c = 1.0 \times 10^{-6} \text{ mol dm}^{-3}$, $\lambda_{\text{exc}}=300 \text{ nm}$) upon titration with poly(dGdC)₂ ($c = 1.0 \times 10^{-6} - 3.1 \times 10^{-5} \text{ mol dm}^{-3}$); b) Dependence of **23** absorbance at $\lambda_{\text{max}} = 372 \text{ nm}$ on $c(\text{poly(dGdC)}_2)$, at pH 7.0, sodium cacodylate buffer, $I = 0.05 \text{ mol dm}^{-3}$.

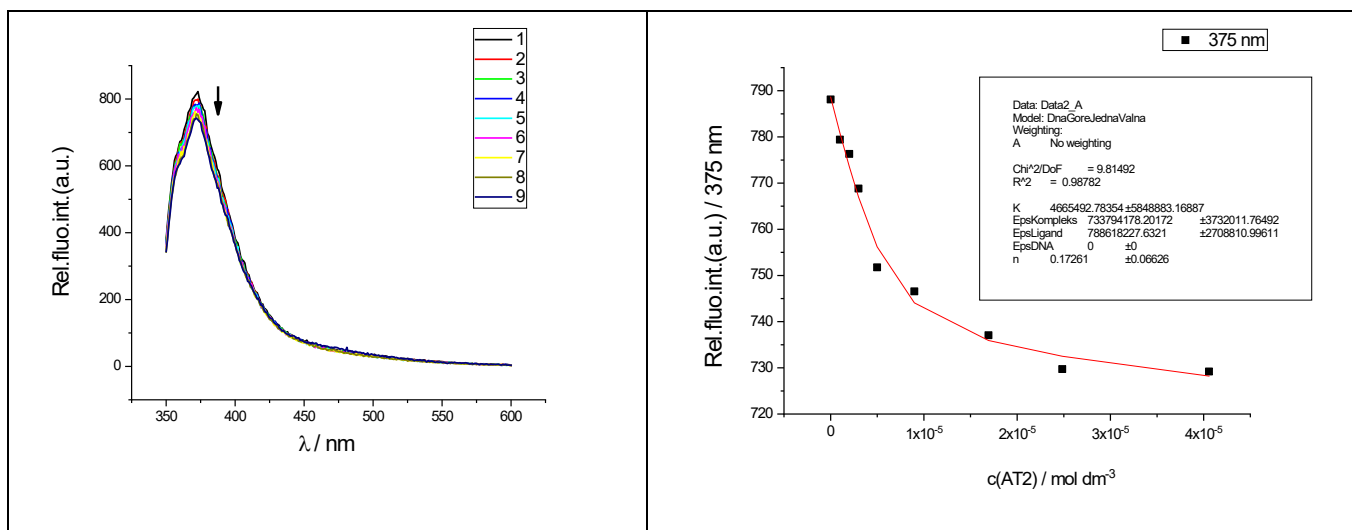


Figure S19. a) Changes in fluorescence spectrum of **23** ($c = 1.0 \times 10^{-6} \text{ mol dm}^{-3}$, $\lambda_{\text{exc}}=300 \text{ nm}$) upon titration with poly(dAdT)₂ ($c = 1.0 \times 10^{-6} - 4.1 \times 10^{-5} \text{ mol dm}^{-3}$); b) Dependence of **23** absorbance at $\lambda_{\text{max}} = 375 \text{ nm}$ on $c(\text{poly(dAdT)}_2)$, at pH 7.0, sodium cacodylate buffer, $I = 0.05 \text{ mol dm}^{-3}$.

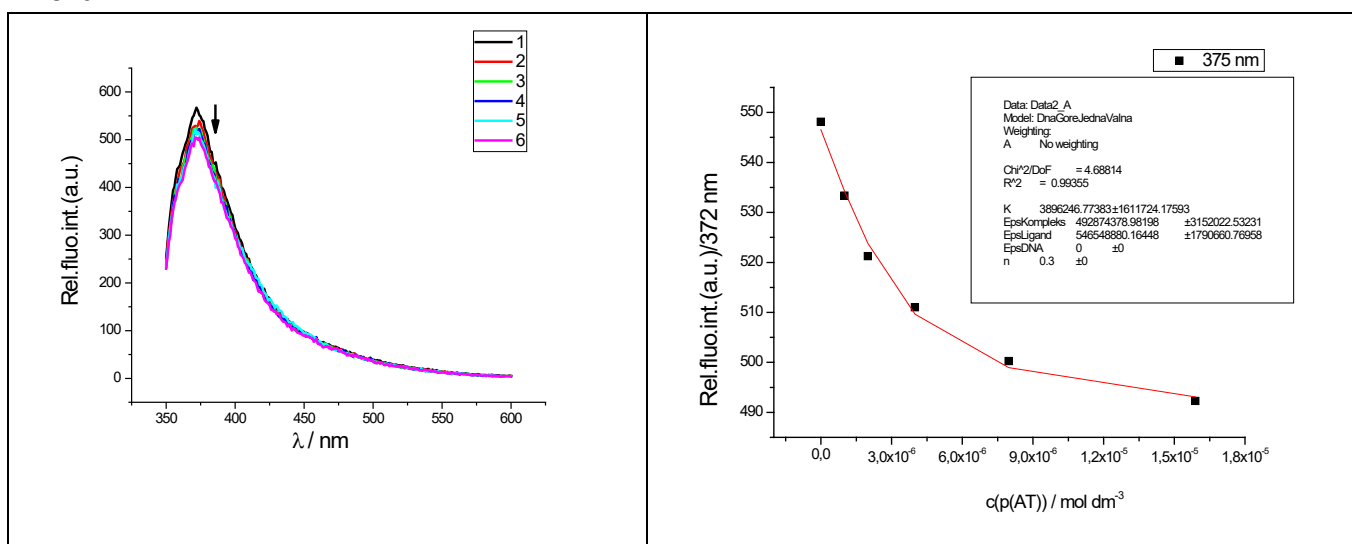


Figure S20. a) Changes in fluorescence spectrum of **23** ($c = 1.0 \times 10^{-6} \text{ mol dm}^{-3}$, $\lambda_{\text{exc}}=300 \text{ nm}$) upon titration with poly dA-poly dT ($c = 1.0 \times 10^{-6} - 1.6 \times 10^{-5} \text{ mol dm}^{-3}$); b) Dependence of **23** absorbance at $\lambda_{\text{max}} = 375 \text{ nm}$ on $c(\text{poly dA-poly dT})$, at pH 7.0, sodium cacodylate buffer, $I = 0.05 \text{ mol dm}^{-3}$.

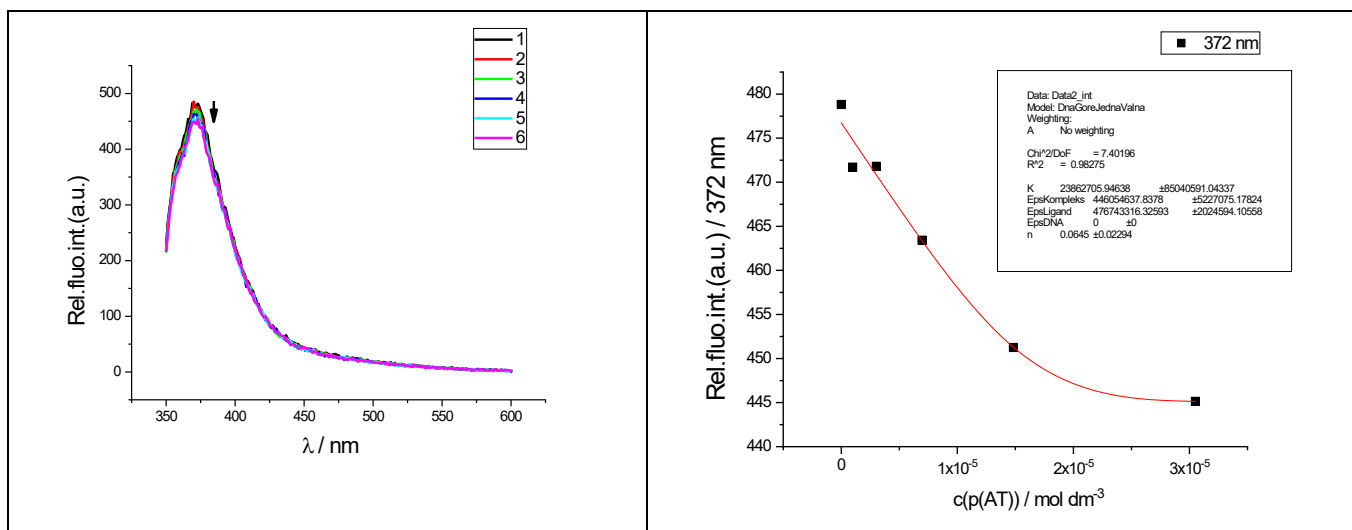


Figure S21. a) Changes in fluorescence spectrum of **23** ($c = 1.0 \times 10^{-6} \text{ mol dm}^{-3}$, $\lambda_{\text{exc}} = 300 \text{ nm}$) upon titration with ATT ($c = 1.0 \times 10^{-6} - 1.6 \times 10^{-5} \text{ mol dm}^{-3}$); b) Dependence of **23** absorbance at $\lambda_{\text{max}} = 372 \text{ nm}$ on $c(\text{ATT})$, at pH 7.0, sodium cacodylate buffer, $I = 0.05 \text{ mol dm}^{-3}$.

2.1.2. Fluorimetric titrations at pH 5.0

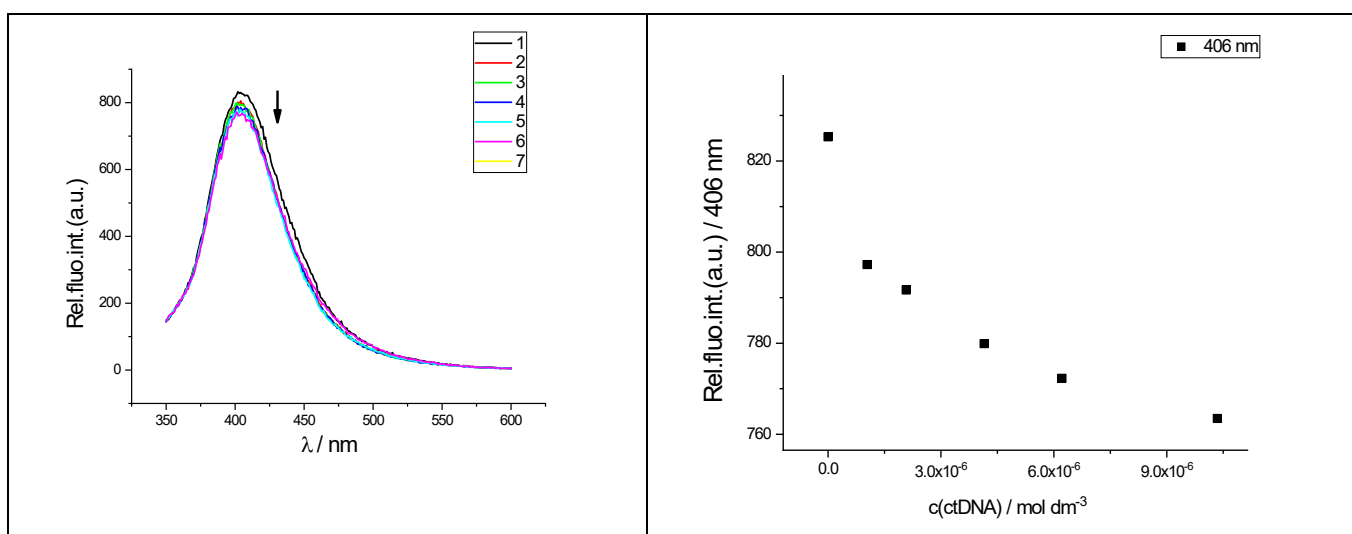


Figure S22. a) Changes in fluorescence spectrum of **19** ($c = 1.0 \times 10^{-6} \text{ mol dm}^{-3}$, $\lambda_{\text{exc}} = 300 \text{ nm}$) upon titration with ctDNA ($c = 1.0 \times 10^{-6} - 1 \times 10^{-5} \text{ mol dm}^{-3}$); b) Dependence of **19** absorbance at $\lambda_{\text{max}} = 406 \text{ nm}$ on $c(\text{ctDNA})$, at pH 5.0, sodium cacodylate buffer, $I = 0.05 \text{ mol dm}^{-3}$.

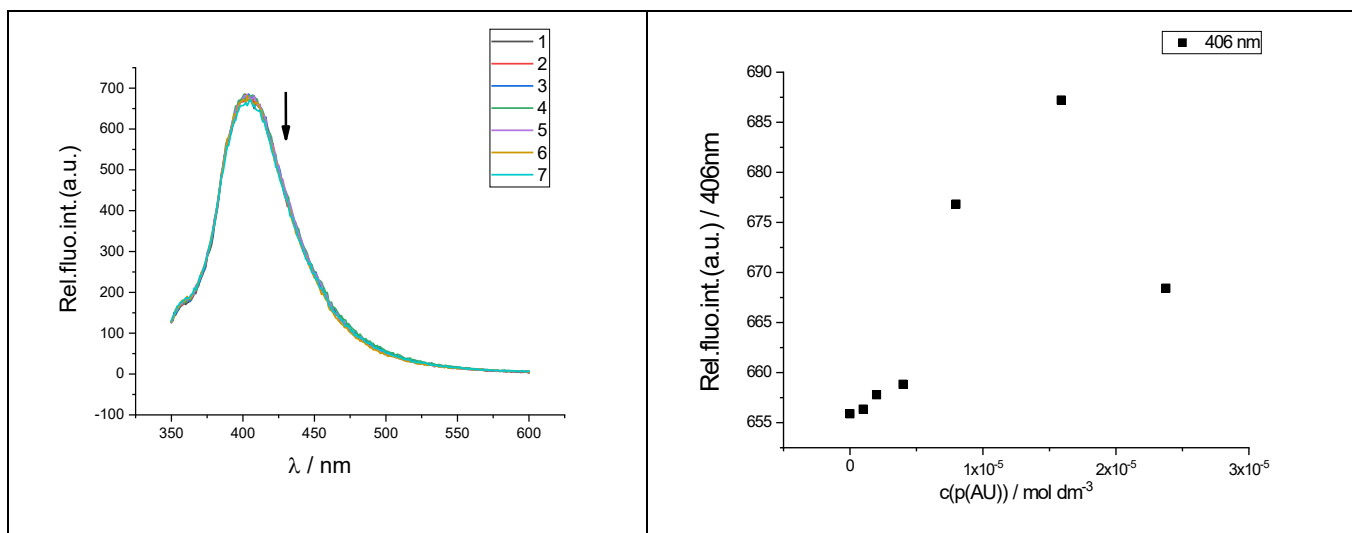


Figure S23. a) Changes in fluorescence spectrum of **19** ($c = 1.0 \times 10^{-6} \text{ mol dm}^{-3}$, $\lambda_{\text{exc}} = 300 \text{ nm}$) upon titration with poly A-poly U ($c = 1.0 \times 10^{-6} - 1.8 \times 10^{-5} \text{ mol dm}^{-3}$); b) Dependence of **19** absorbance at $\lambda_{\text{max}} = 406 \text{ nm}$ on $c(\text{poly A-poly U})$, at pH 5.0, sodium cacodylate buffer, $I = 0.05 \text{ mol dm}^{-3}$.

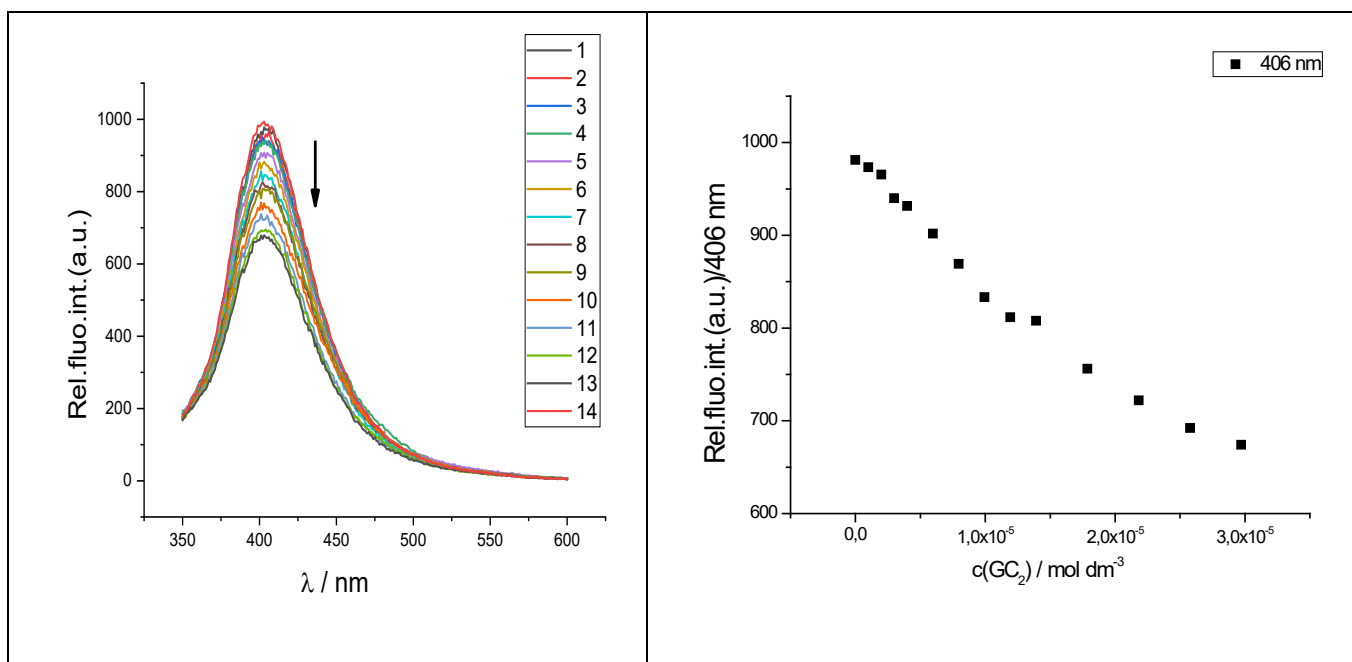


Figure S24. a) Changes in fluorescence spectrum of **19** ($c = 1.0 \times 10^{-6} \text{ mol dm}^{-3}$, $\lambda_{\text{exc}} = 300 \text{ nm}$) upon titration with poly(dGdC)₂ ($c = 1.0 \times 10^{-6} - 2.9 \times 10^{-5} \text{ mol dm}^{-3}$); b) Dependence of **19** absorbance at $\lambda_{\text{max}} = 406 \text{ nm}$ on $c(\text{poly(dGdC)}_2)$, at pH 5.0, sodium cacodylate buffer, $I = 0.05 \text{ mol dm}^{-3}$.

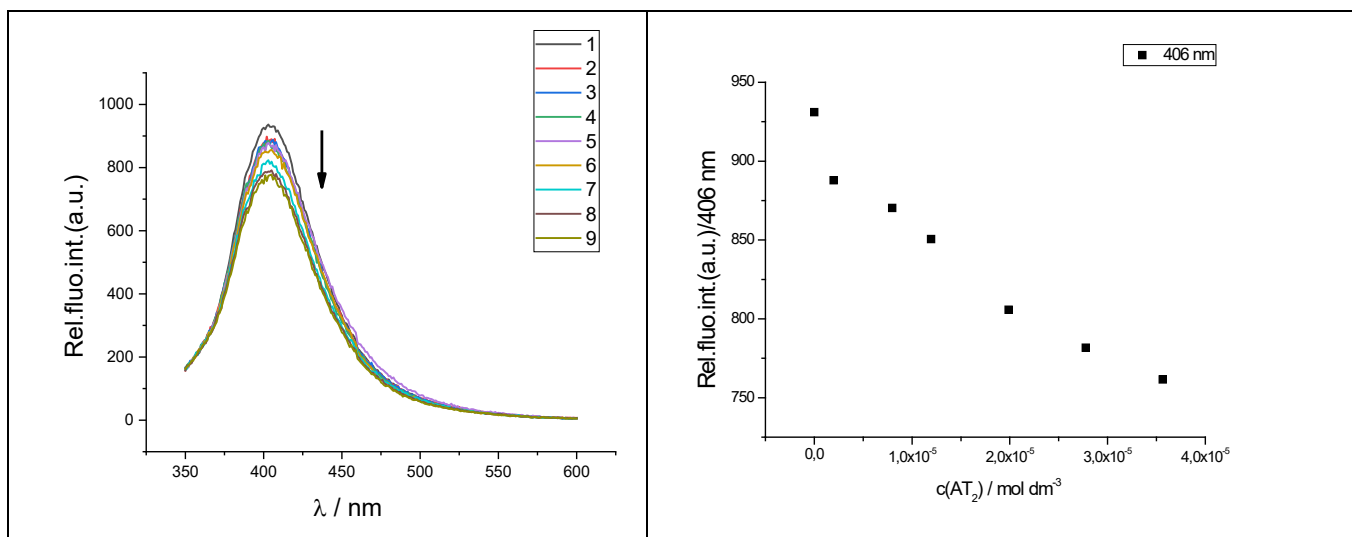


Figure S25. a) Changes in fluorescence spectrum of **19** ($c = 1.0 \times 10^{-6} \text{ mol dm}^{-3}$, $\lambda_{\text{exc}} = 300 \text{ nm}$) upon titration with poly(dAdT)₂ ($c = 1.0 \times 10^{-6} - 3.6 \times 10^{-5} \text{ mol dm}^{-3}$); b) Dependence of **19** absorbance at $\lambda_{\text{max}} = 406 \text{ nm}$ on $c(\text{poly(dAdT)}_2)$, at pH 5.0, sodium cacodylate buffer, $I = 0.05 \text{ mol dm}^{-3}$.

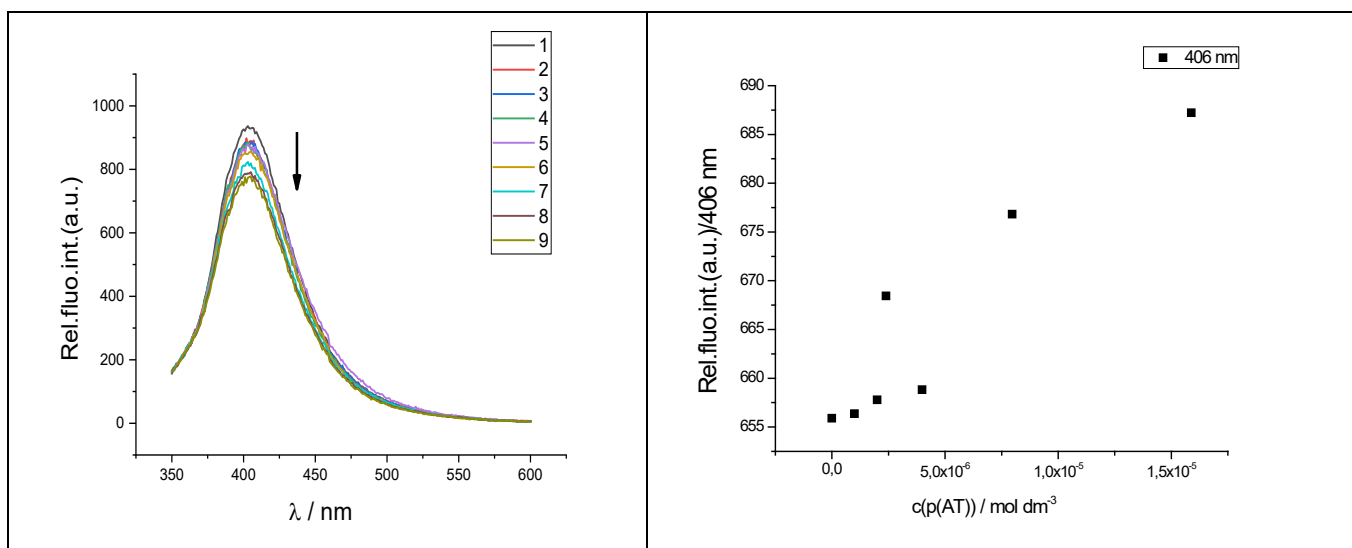


Figure S26. a) Changes in fluorescence spectrum of **19** ($c = 1.0 \times 10^{-6} \text{ mol dm}^{-3}$, $\lambda_{\text{exc}} = 300 \text{ nm}$) upon titration with poly dA-poly dT ($c = 1.0 \times 10^{-6} - 3.6 \times 10^{-5} \text{ mol dm}^{-3}$); b) Dependence of **19** absorbance at $\lambda_{\text{max}} = 406 \text{ nm}$ on $c(\text{poly dA-poly dT})$, at pH 5.0, sodium cacodylate buffer, $I = 0.05 \text{ mol dm}^{-3}$.

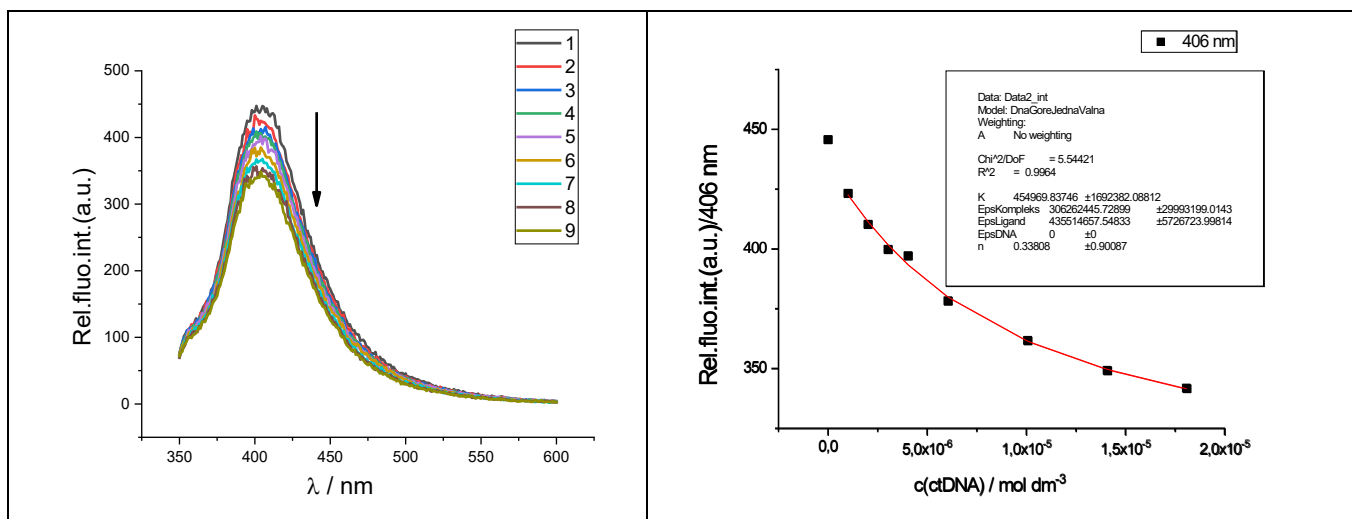


Figure S27. a) Changes in fluorescence spectrum of **22** ($c = 1.0 \times 10^{-6} \text{ mol dm}^{-3}$, $\lambda_{\text{exc}}=300 \text{ nm}$) upon titration with ctDNA ($c = 1.0 \times 10^{-6} - 1.8 \times 10^{-5} \text{ mol dm}^{-3}$); b) Dependence of **22** absorbance at $\lambda_{\text{max}} = 406 \text{ nm}$ on $c(\text{ctDNA})$, at pH 5.0, sodium cacodylate buffer, $I = 0.05 \text{ mol dm}^{-3}$.

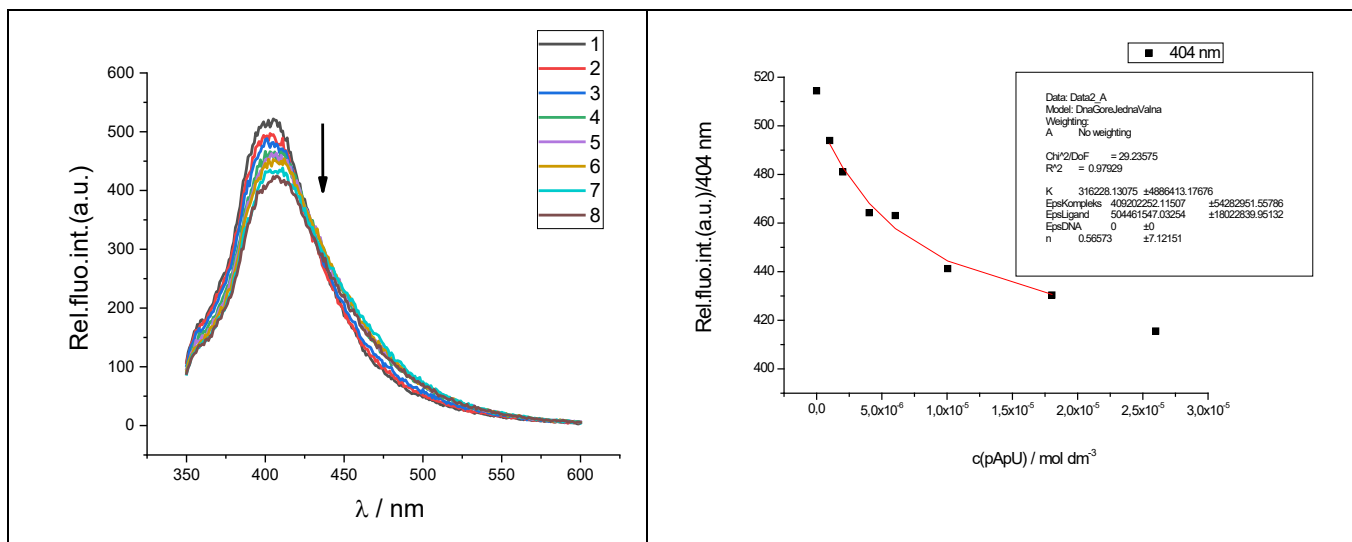


Figure S28. a) Changes in fluorescence spectrum of **22** ($c = 1.0 \times 10^{-6} \text{ mol dm}^{-3}$, $\lambda_{\text{exc}}=300 \text{ nm}$) upon titration with poly A-poly U ($c = 1.0 \times 10^{-6} - 2.6 \times 10^{-5} \text{ mol dm}^{-3}$); b) Dependence of **22** absorbance at $\lambda_{\text{max}} = 473 \text{ nm}$ on $c(\text{poly A-poly U})$, at pH 5.0, sodium cacodylate buffer, $I = 0.05 \text{ mol dm}^{-3}$.

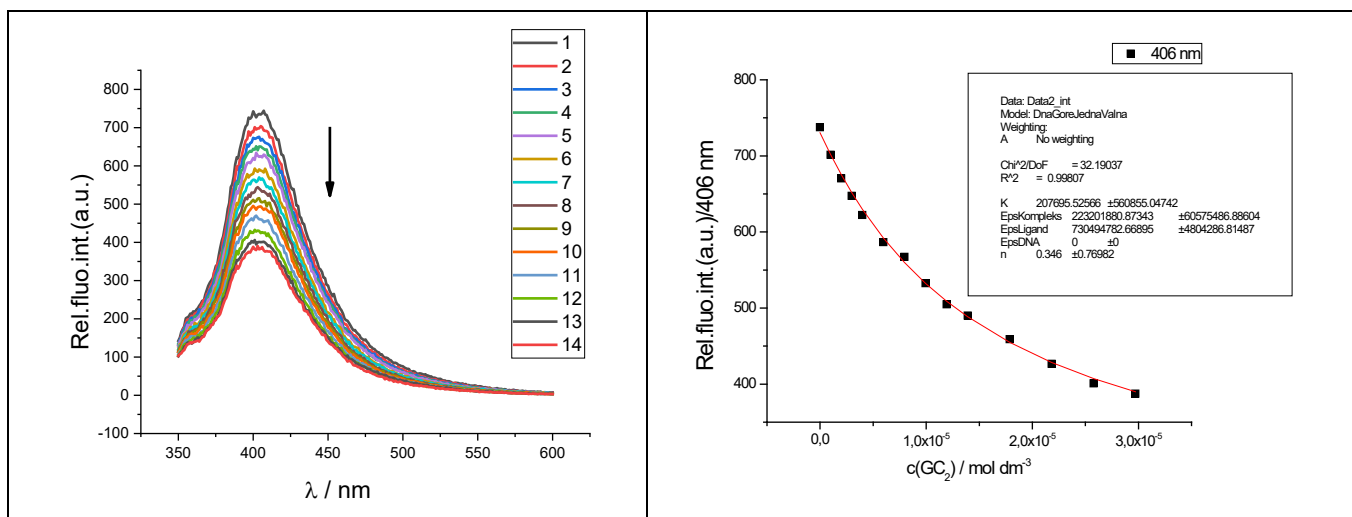


Figure S29. a) Changes in fluorescence spectrum of **22** ($c = 1.0 \times 10^{-6} \text{ mol dm}^{-3}$, $\lambda_{\text{exc}} = 300 \text{ nm}$) upon titration with poly(dGdC)₂ ($c = 9.9 \times 10^{-7} - 2.9 \times 10^{-5} \text{ mol dm}^{-3}$); b) Dependence of **22** absorbance at $\lambda_{\text{max}} = 406 \text{ nm}$ on $c(\text{poly}(\text{dGdC})_2)$, at pH 5.0, sodium cacodylate buffer, $I = 0.05 \text{ mol dm}^{-3}$.

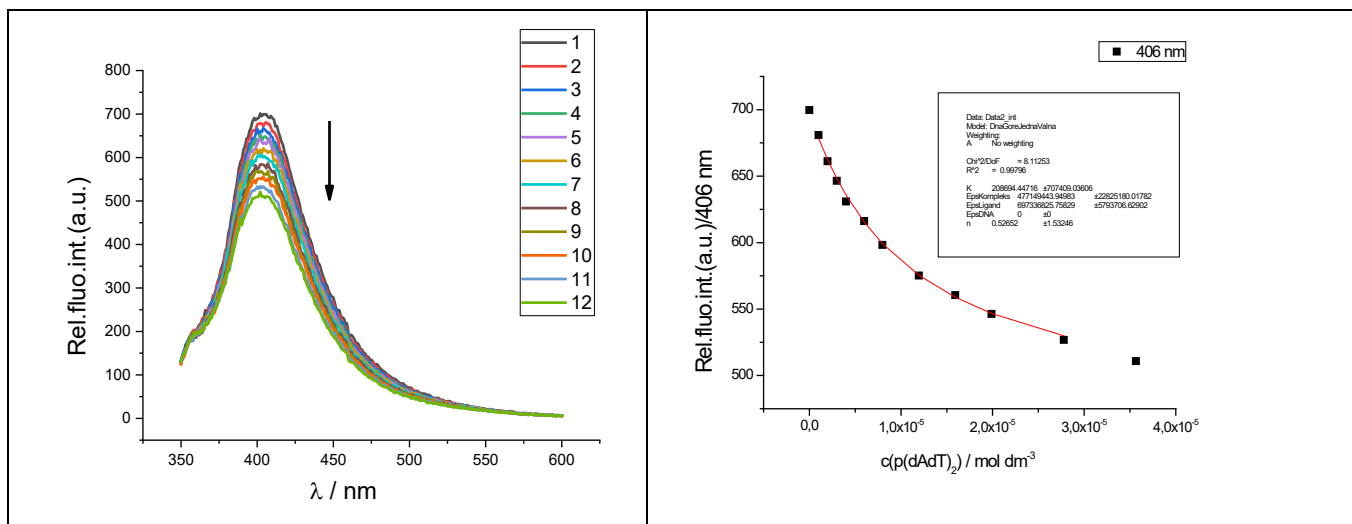


Figure S30. a) Changes in fluorescence spectrum of **22** ($c = 1.0 \times 10^{-6} \text{ mol dm}^{-3}$, $\lambda_{\text{exc}} = 300 \text{ nm}$) upon titration with poly(dAdT)₂ ($c = 1.0 \times 10^{-6} - 3.6 \times 10^{-5} \text{ mol dm}^{-3}$); b) Dependence of **22** absorbance at $\lambda_{\text{max}} = 406 \text{ nm}$ on $c(\text{poly}(\text{dAdT})_2)$, at pH 5.0, sodium cacodylate buffer, $I = 0.05 \text{ mol dm}^{-3}$.

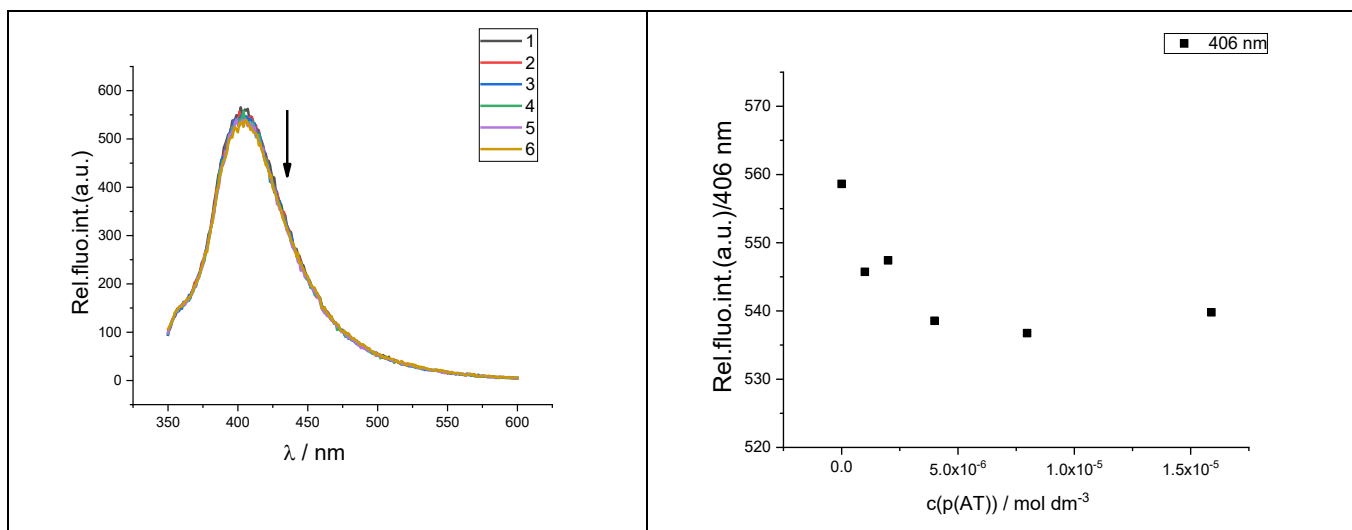


Figure S31. a) Changes in fluorescence spectrum of **22** ($c = 1.0 \times 10^{-6} \text{ mol dm}^{-3}$, $\lambda_{\text{exc}} = 300 \text{ nm}$) upon titration with poly dA-poly dT ($c = 1.0 \times 10^{-6} - 1.6 \times 10^{-5} \text{ mol dm}^{-3}$); b) Dependence of **22** absorbance at $\lambda_{\text{max}} = 406 \text{ nm}$ on $c(\text{poly dA-poly dT})$, at pH 5.0, sodium cacodylate buffer, $I = 0.05 \text{ mol dm}^{-3}$.

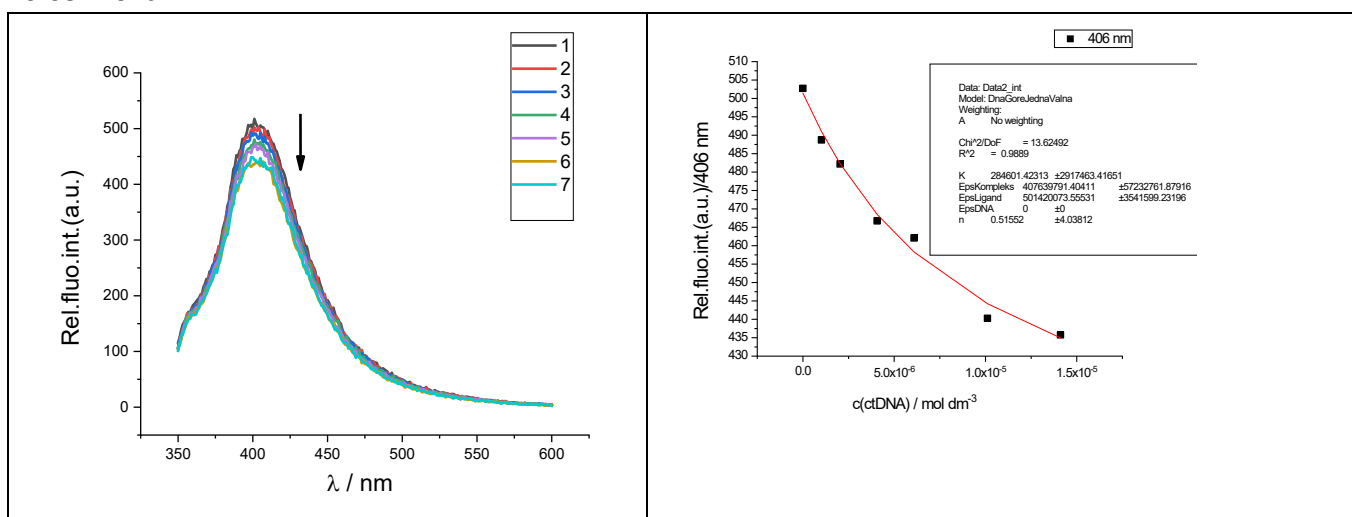


Figure S32. a) Changes in fluorescence spectrum of **23** ($c = 1.0 \times 10^{-6} \text{ mol dm}^{-3}$, $\lambda_{\text{exc}} = 300 \text{ nm}$) upon titration with ctDNA ($c = 1.0 \times 10^{-6} - 1.4 \times 10^{-5} \text{ mol dm}^{-3}$); b) Dependence of **23** absorbance at $\lambda_{\text{max}} = 406 \text{ nm}$ on $c(\text{ctDNA})$, at pH 5.0, sodium cacodylate buffer, $I = 0.05 \text{ mol dm}^{-3}$.

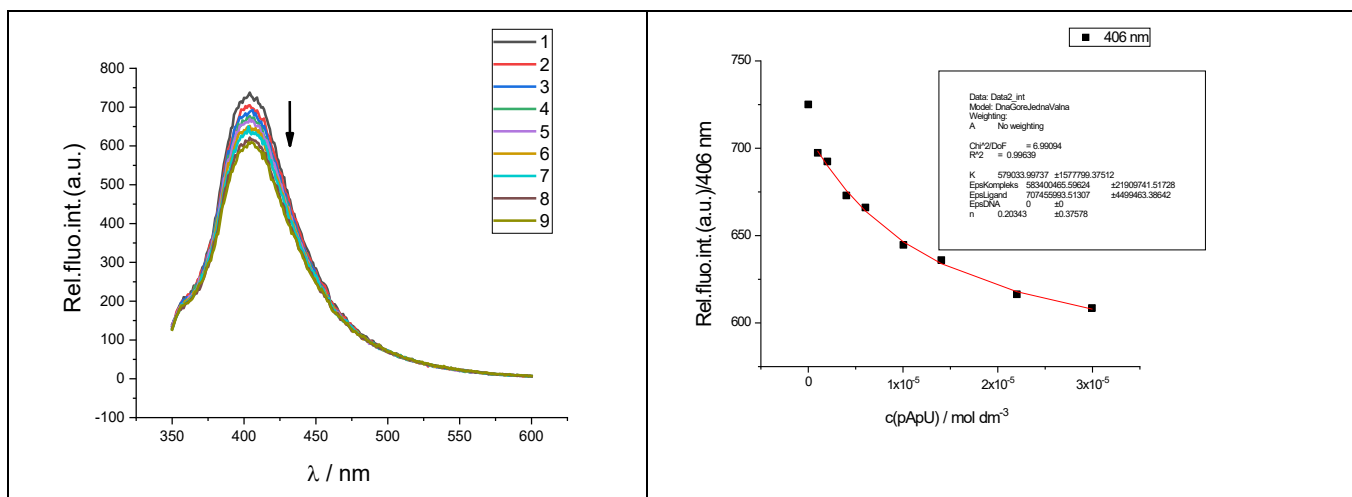


Figure S33. a) Changes in fluorescence spectrum of **23** ($c = 1.0 \times 10^{-6} \text{ mol dm}^{-3}$, $\lambda_{\text{exc}}=300 \text{ nm}$) upon titration with poly A-poly U ($c = 1.0 \times 10^{-6} - 2.99 \times 10^{-5} \text{ mol dm}^{-3}$); b) Dependence of **23** absorbance at $\lambda_{\text{max}} = 406 \text{ nm}$ on $c(\text{poly A-poly U})$, at pH 5.0, sodium cacodylate buffer, $I = 0.05 \text{ mol dm}^{-3}$.

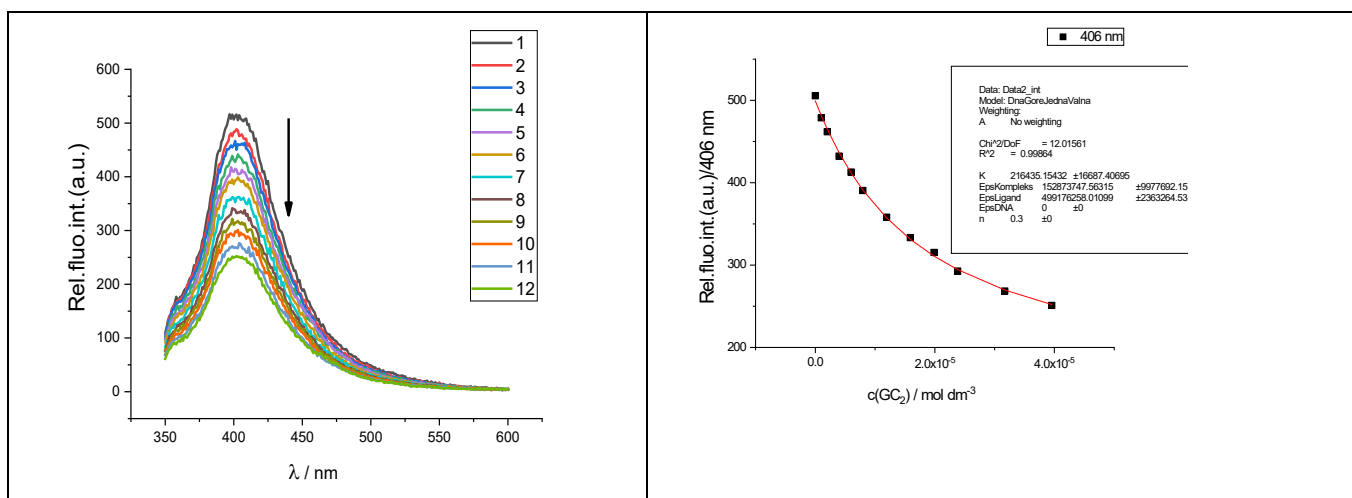


Figure S34. a) Changes in fluorescence spectrum of **23** ($c = 1.0 \times 10^{-6} \text{ mol dm}^{-3}$, $\lambda_{\text{exc}}=300 \text{ nm}$) upon titration with poly(dGdC)₂ ($c = 1.0 \times 10^{-6} - 3.96 \times 10^{-5} \text{ mol dm}^{-3}$); b) Dependence of **23** absorbance at $\lambda_{\text{max}} = 406 \text{ nm}$ on $c(\text{poly(dGdC)}_2)$, at pH 5.0, sodium cacodylate buffer, $I = 0.05 \text{ mol dm}^{-3}$.

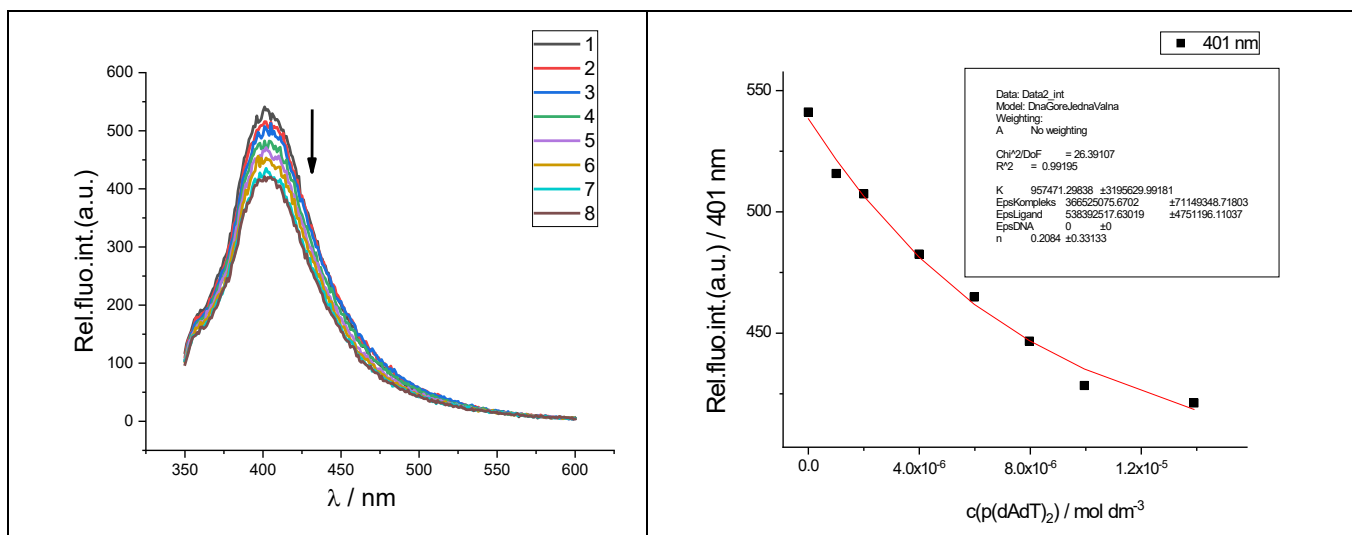


Figure S35. a) Changes in fluorescence spectrum of **23** ($c = 1.0 \times 10^{-6} \text{ mol dm}^{-3}$, $\lambda_{\text{exc}}=300 \text{ nm}$) upon titration with poly(dAdT)₂ ($c = 1.0 \times 10^{-6} - 1.39 \times 10^{-5} \text{ mol dm}^{-3}$); b) Dependence of **23** absorbance at $\lambda_{\text{max}} = 401 \text{ nm}$ on $c(\text{poly(dAdT)}_2)$, at pH 5.0, sodium cacodylate buffer, $I = 0.05 \text{ mol dm}^{-3}$.

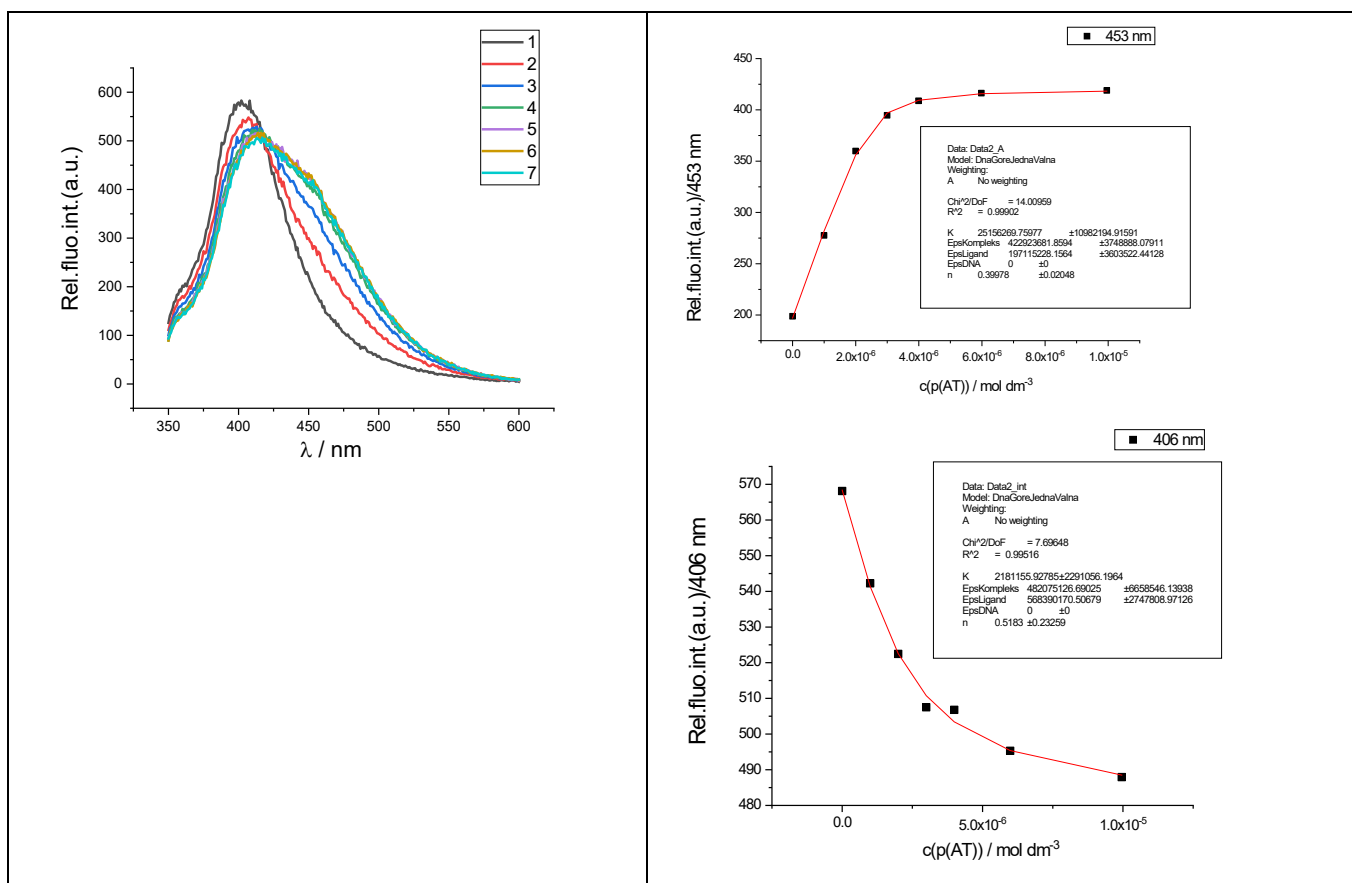


Figure S36. a) Changes in fluorescence spectrum of **23** ($c = 1.0 \times 10^{-6} \text{ mol dm}^{-3}$, $\lambda_{\text{exc}}=300 \text{ nm}$) upon titration with poly dA-poly dT ($c = 1.0 \times 10^{-6} - 9.96 \times 10^{-6} \text{ mol dm}^{-3}$); b) Dependence of **23** absorbance at $\lambda_{\text{max}} = 406 \text{ nm}$ and 453 nm on $c(\text{poly dA-poly dT})$, at pH 5.0, sodium cacodylate buffer, $I = 0.05 \text{ mol dm}^{-3}$.

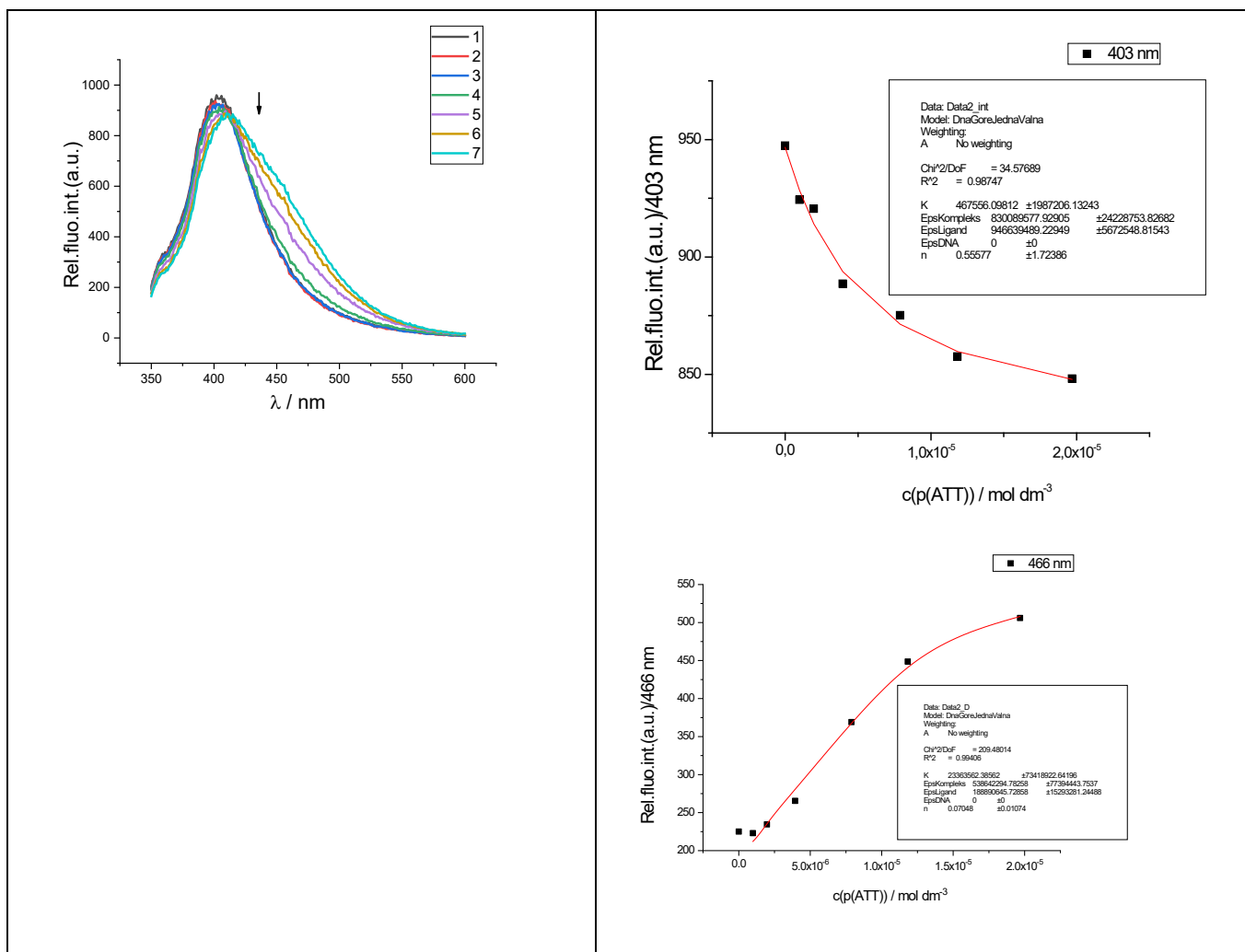
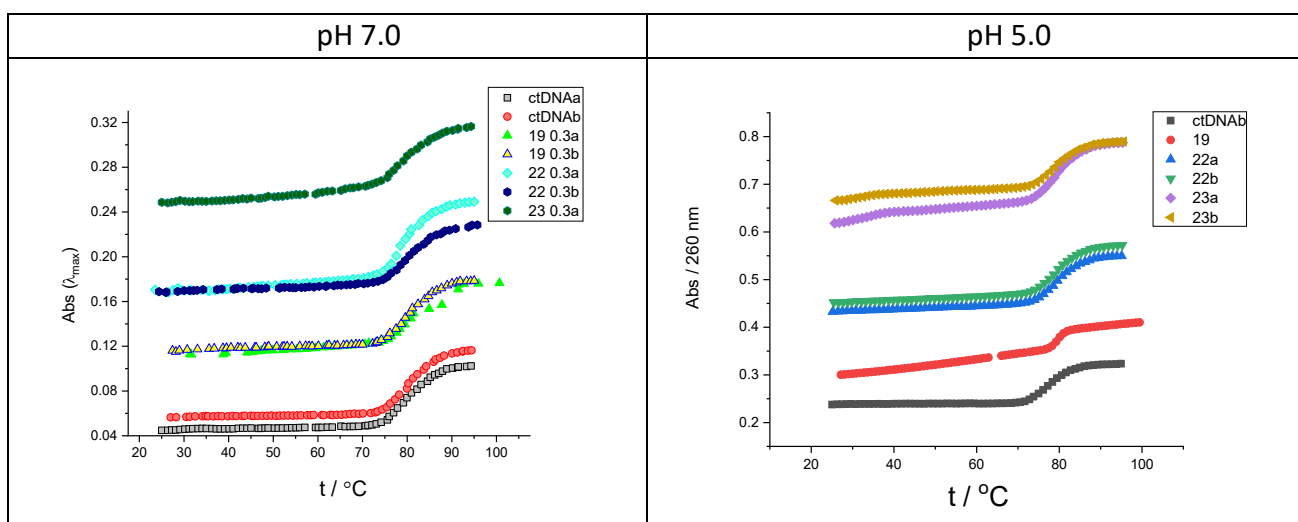


Figure S37. a) Changes in fluorescence spectrum of **23** ($c = 1.0 \times 10^{-6}$ mol dm⁻³, $\lambda_{\text{exc}} = 300$ nm) upon titration with ATT ($c = 1.0 \times 10^{-6} - 1.97 \times 10^{-5}$ mol dm⁻³); b) Dependence of **23** absorbance at $\lambda_{\text{max}} = 403$ nm and 466 nm on $c(\text{ATT})$, at pH 5.0, sodium cacodylate buffer, $I = 0.05$ mol dm⁻³.

2.2. Thermal melting experiments



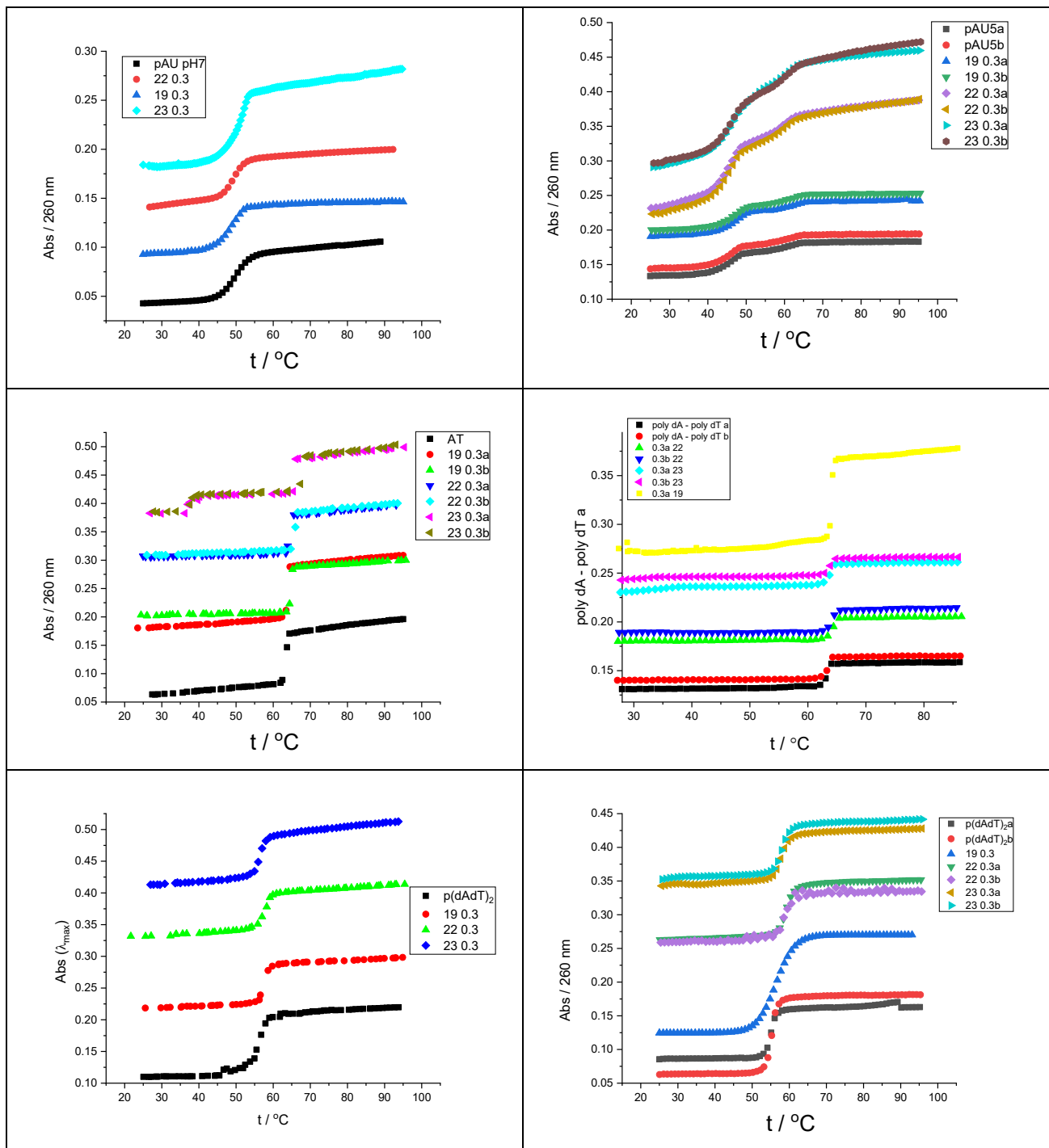


Figure S38. Melting curve of ctDNA, poly A-poly U, poly dA-poly dT, poly (dA-dT)₂ upon addition of ratio, r ([compound]/[polynucleotide])=0.3 of **19**, **22** and **23** at pH = 7.0 and pH = 5.0 (buffer sodium cacodylate, $I = 0.05 \text{ mol dm}^{-3}$).

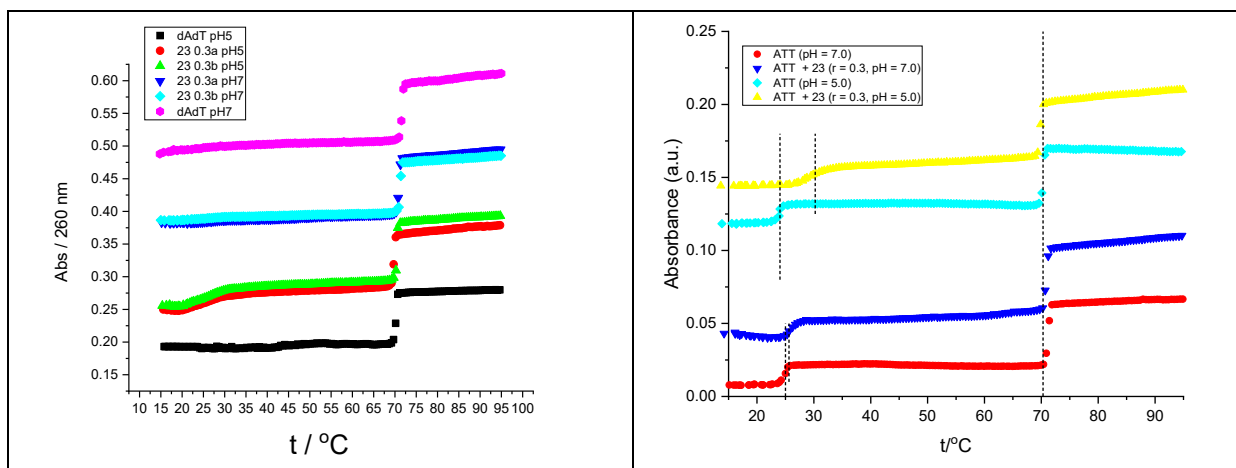
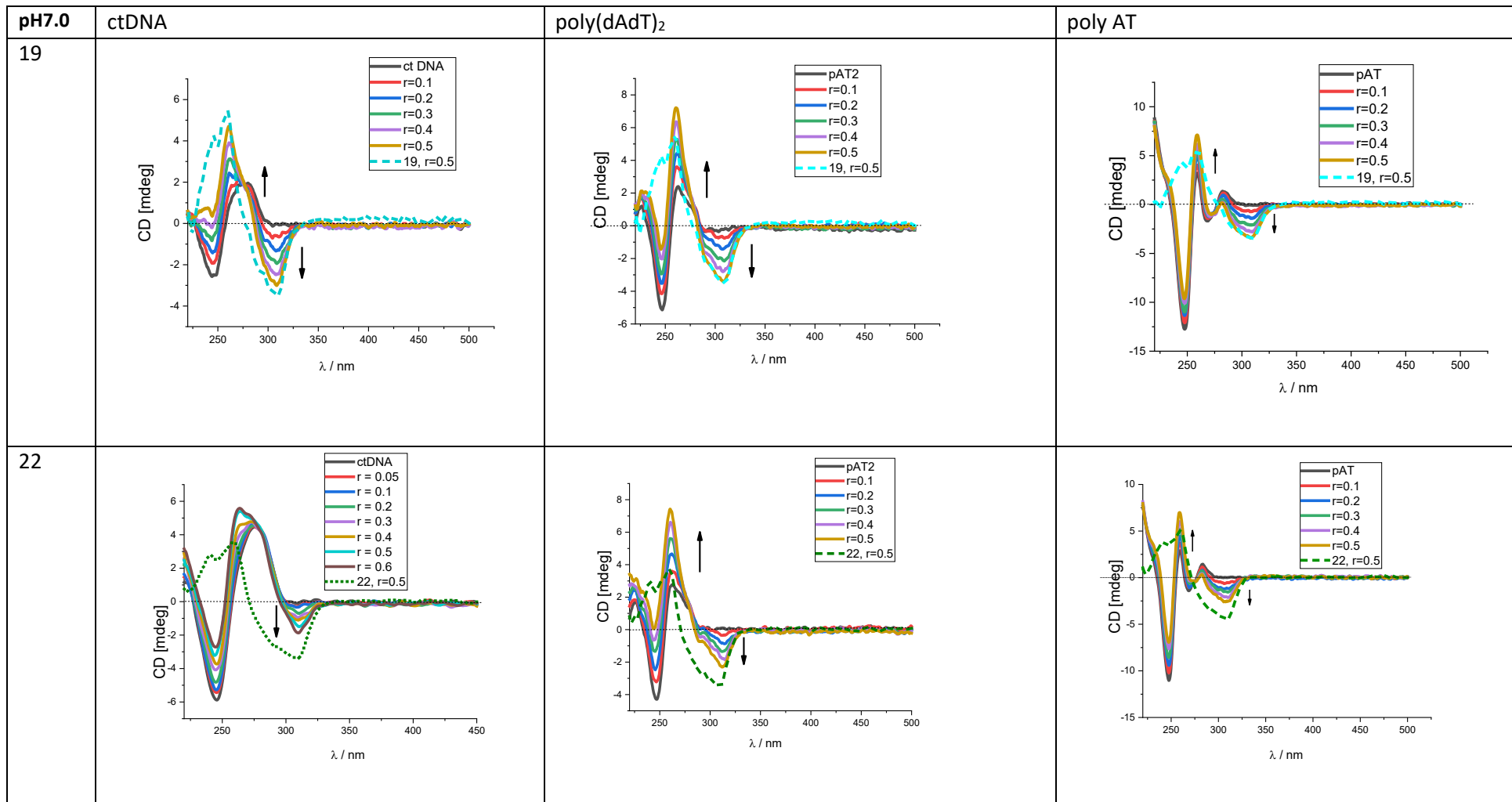
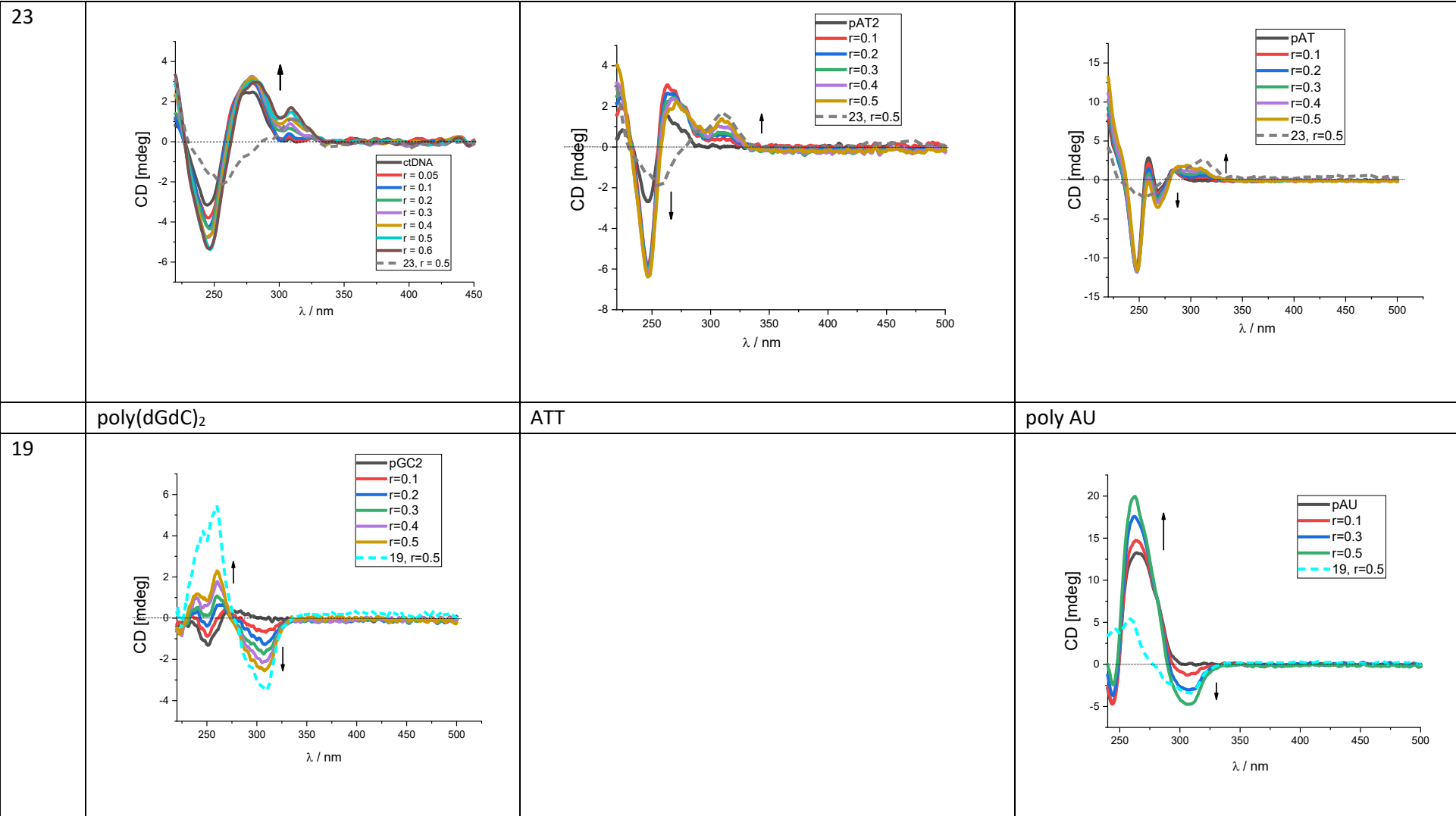


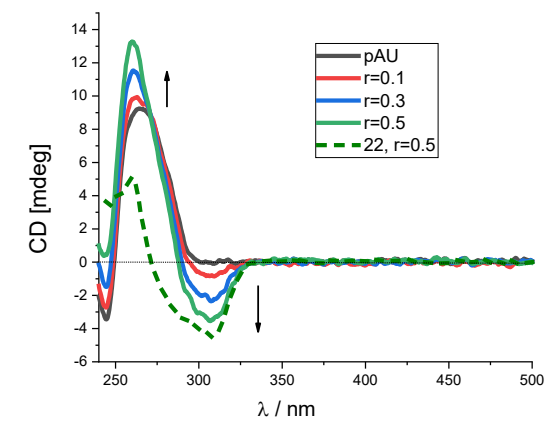
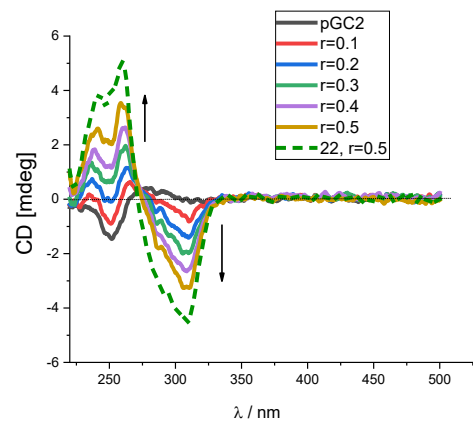
Figure S39. Melting curve of **poly dA-poly dT** and **dAdTdT** upon addition of ratio, r ($[\text{compound}] / [\text{polynucleotide}] = 0.3$) of **23** at pH = 7.0 and pH = 5.0 (buffer sodium cacodylate, $I = 0.1 \text{ mol dm}^{-3}$)

2.3. Circular dichroism (CD) experiments

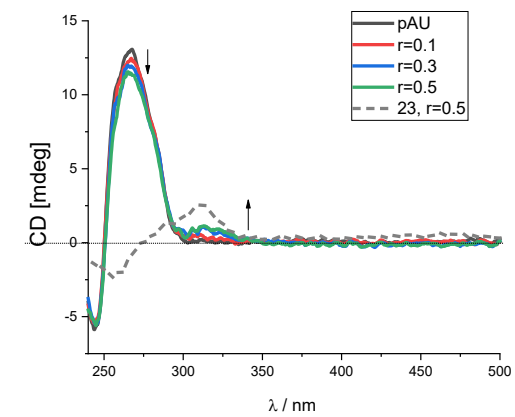
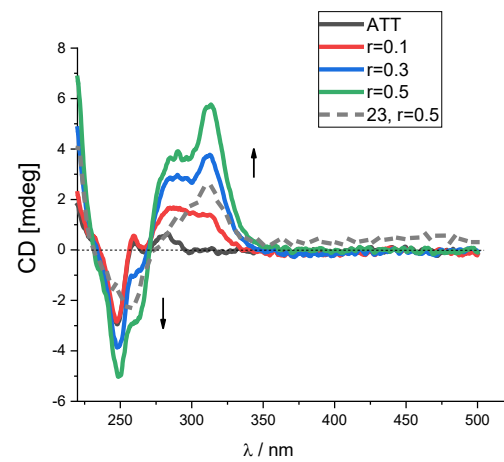
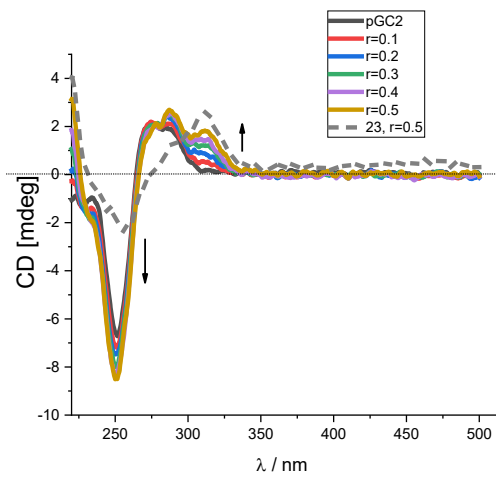


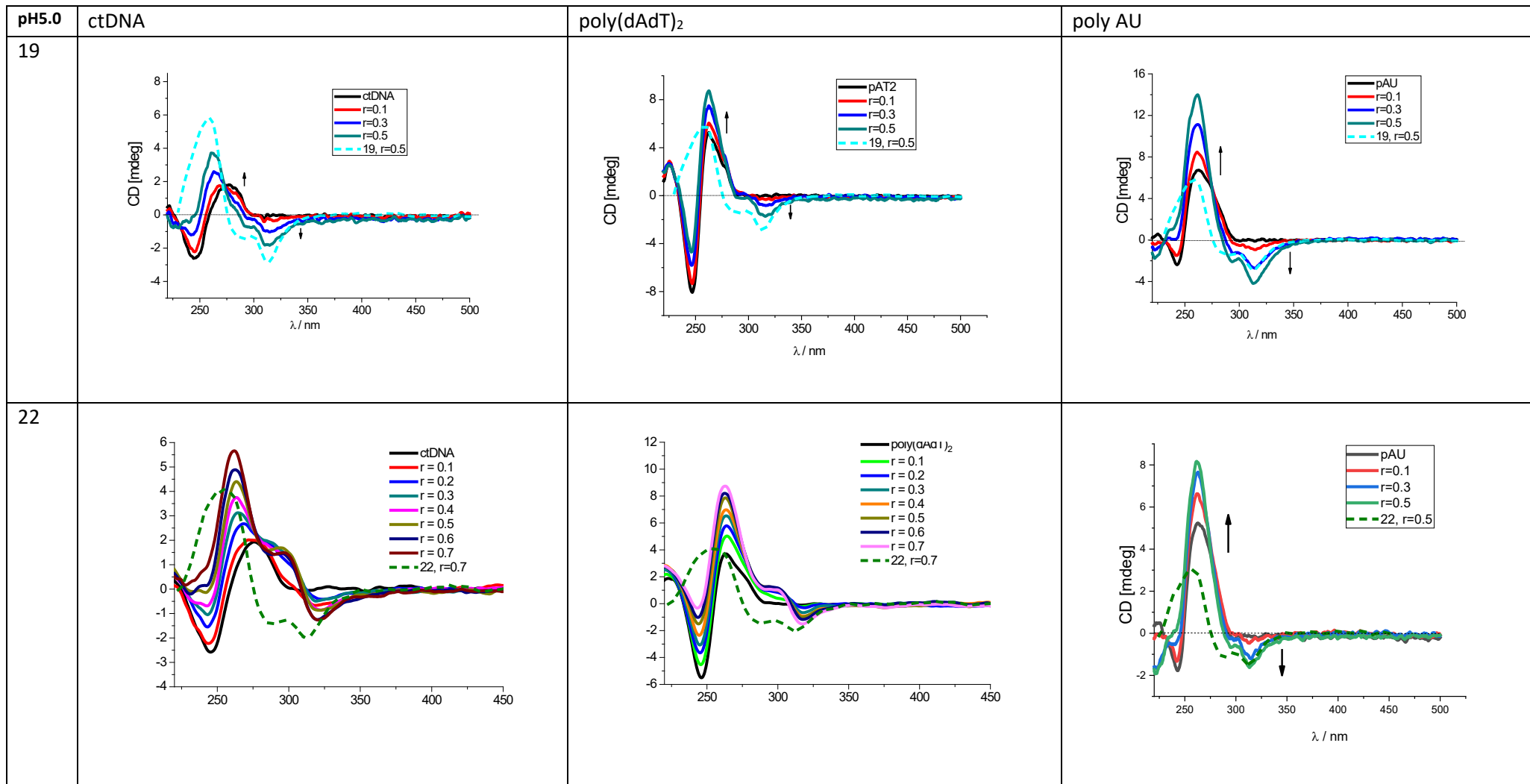


22

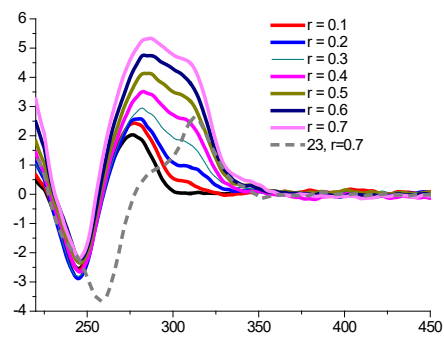
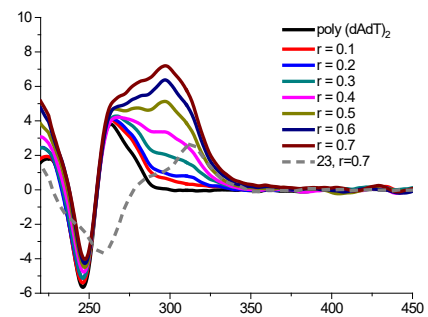


23

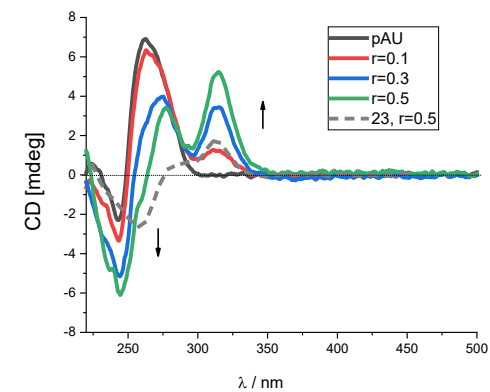




23

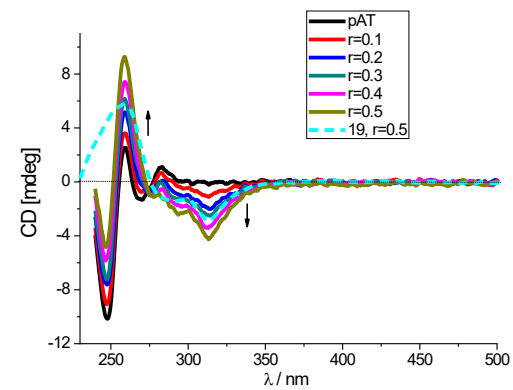
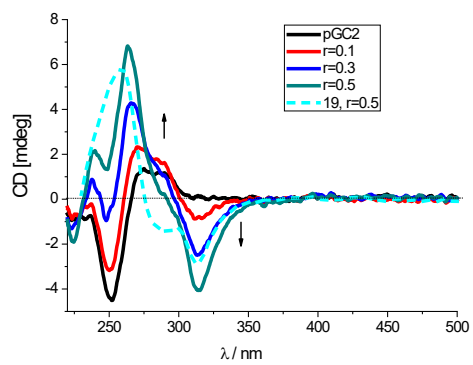
poly(dGdC)₂

ATT



poly AT

19



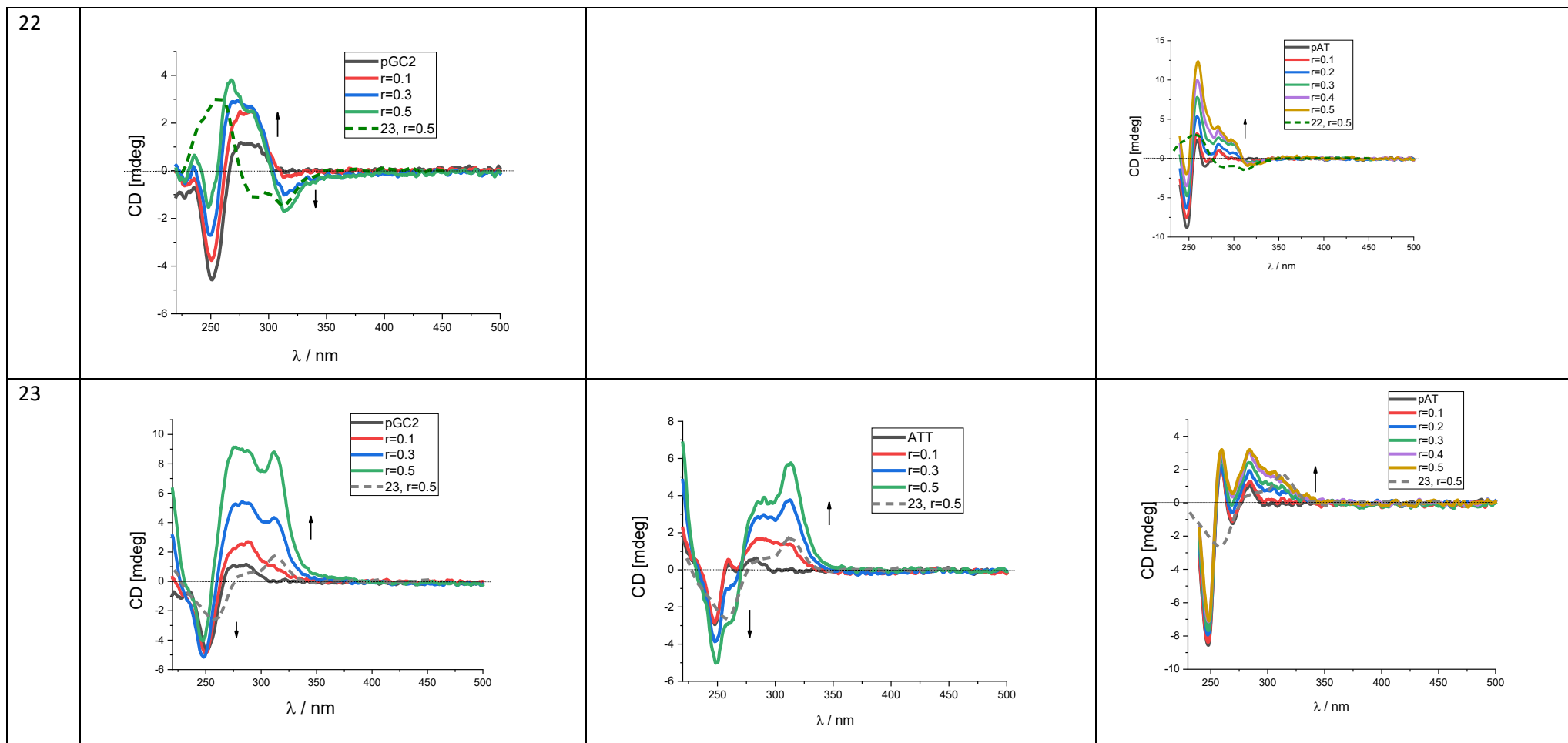


Figure S40. CD titration of polynucleotides ($c = 3.0 \times 10^{-5} \text{ mol dm}^{-3}$) with **19**, **22** and **23** at molar ratios $r = [\text{compound}] / [\text{polynucleotide}]$ (pH = 7.0 and 5.0, buffer sodium cacodylate, $I = 0.05 \text{ mol dm}^{-3}$).

2.4. Mass spectra

2.4. Mass spectra

Figure S41 **a**. Snapshot scan of compound **19** (signal at m/z 587 assigned as $[19+H]^+$ ion) dissolved in H_2O or D_2O about $10^{-5}M$. The observed signals correspond to the H/D exchange results observed for the single charged ion of compound **19**.

0.4

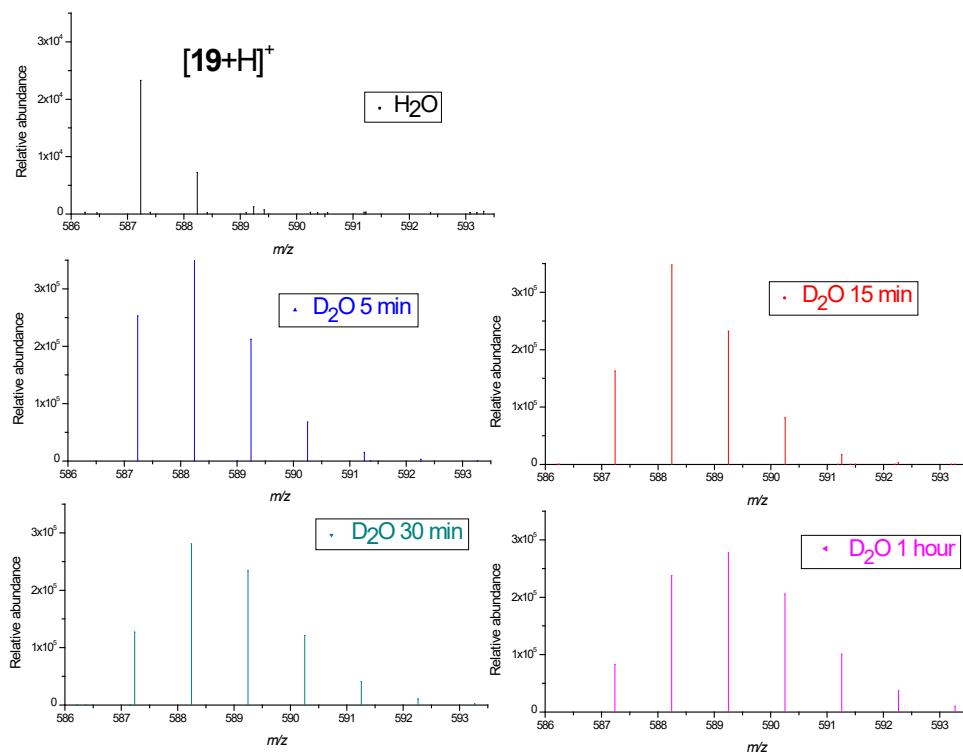


Figure S41 **b**. Snapshot scan of compound **19** (signal at m/z 294 assigned as $[\mathbf{19}+2\text{H}]^{2+}$ ion) dissolved in H_2O or D_2O about 10^{-5}M . The observed signals correspond to the H/D exchange results observed for the double charged ion of compound **19**.

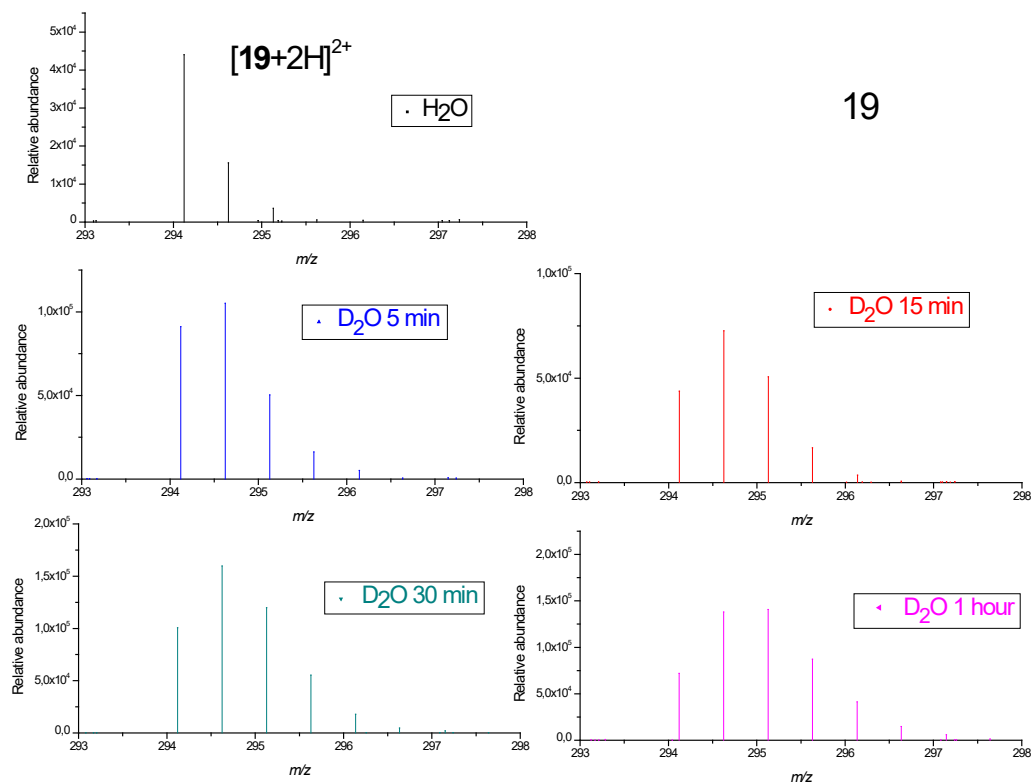


Figure S41 c. Snapshot scan of compound **22** (signal at m/z 658 assigned as $[22+H]^+$ ion) dissolved in H_2O or D_2O about $10^{-5}M$. The observed signals correspond to the H/D exchange results observed for the single charged ion of compound **22**.

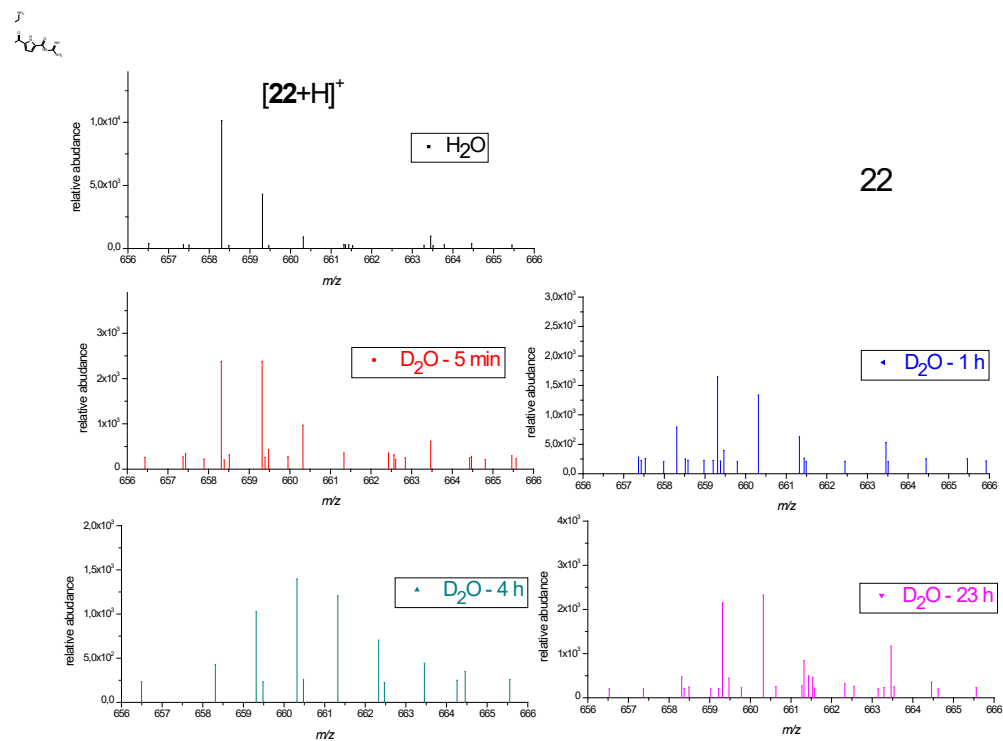


Figure S41 d. Snapshot scan of compound **22** (signal at m/z 329 assigned as $[\mathbf{22}+2\text{H}]^{2+}$ ion) dissolved in H_2O or D_2O about 10^{-5}M . The observed signals correspond to the H/D exchange results observed for the double charged ion of compound **22**.

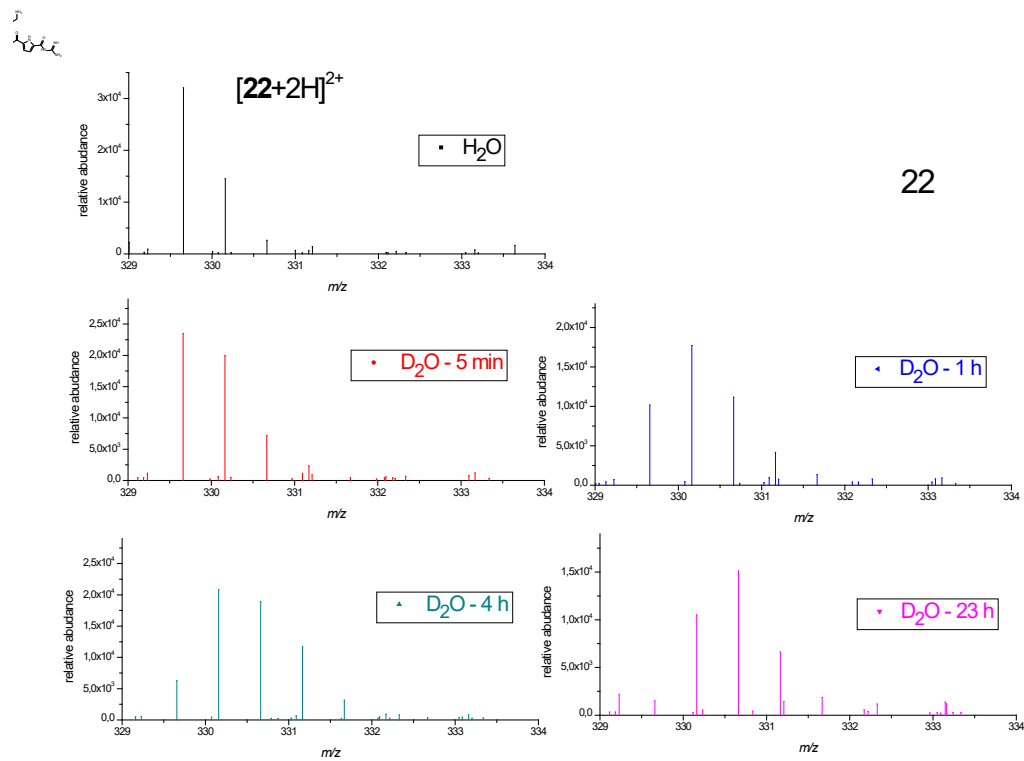


Figure S41 e. Snapshot scan of compound **23** (signal at m/z 658 assigned as $[23+H]^+$ ion) dissolved in H_2O or D_2O about $10^{-5}M$. The observed signals correspond to the H/D exchange results observed for the single charged ion of compound **23**.

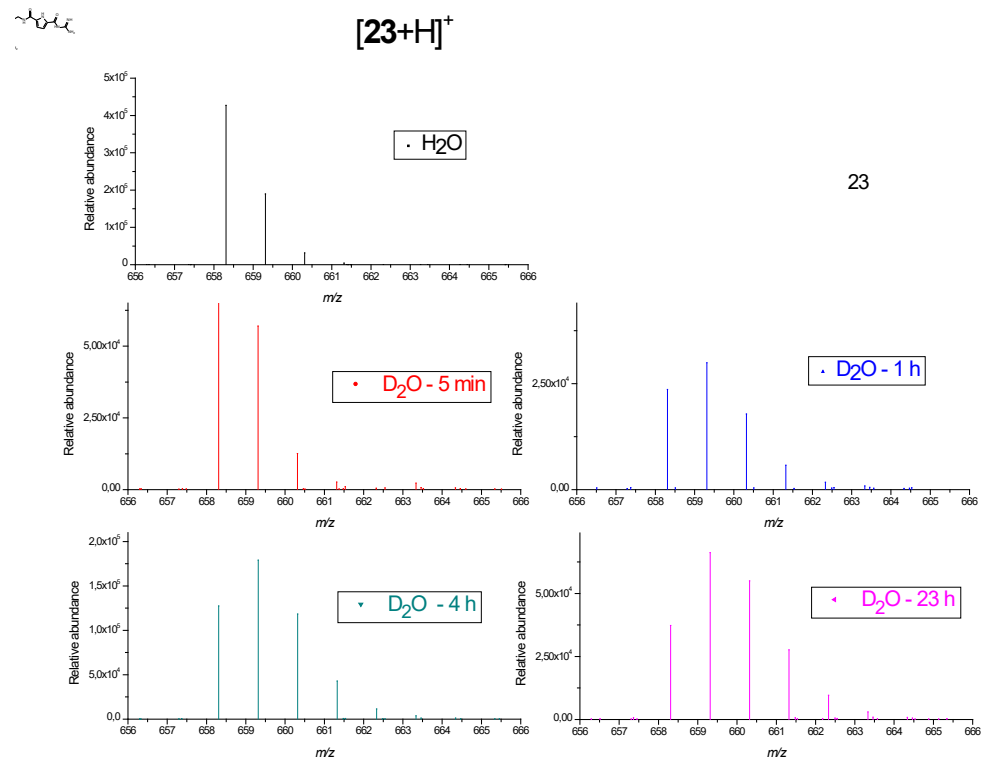


Figure S41 f. Snapshot scan of compound **23** (signal at m/z 329 assigned as $[\mathbf{23}+2\text{H}]^{2+}$ ion) dissolved in H_2O or D_2O about 10^{-5}M . The observed signals correspond to the H/D exchange results observed for the double-charged ion of compound **23**.

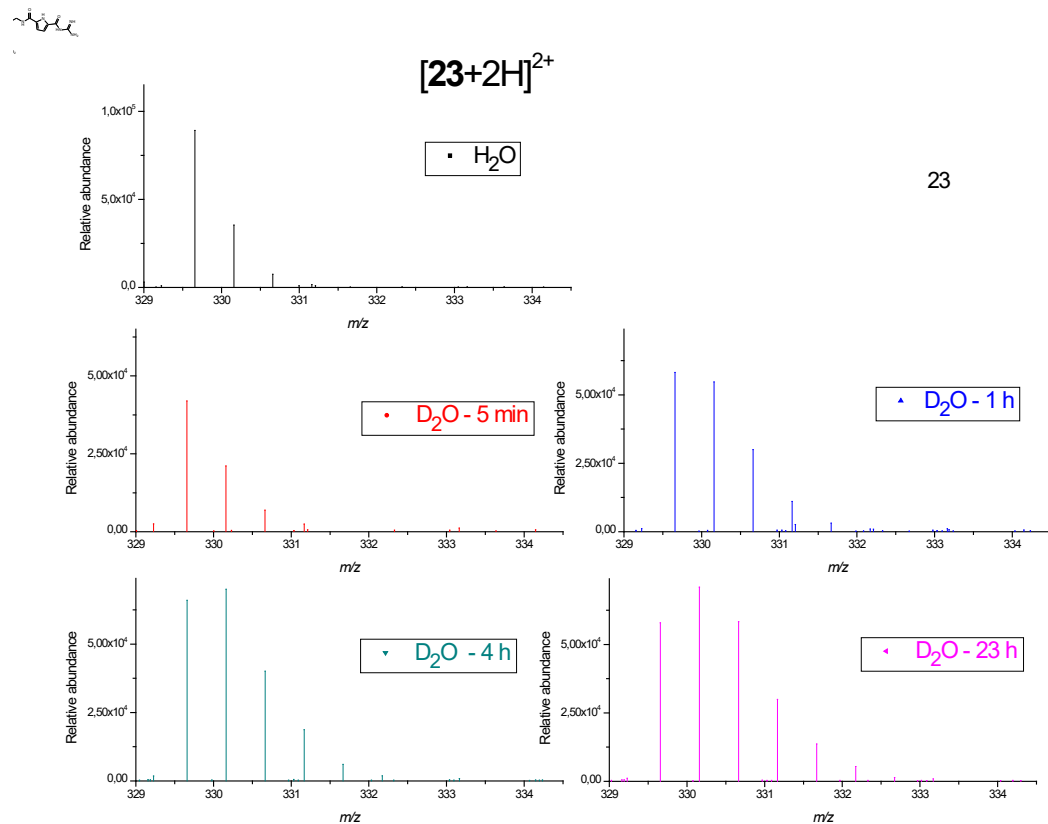
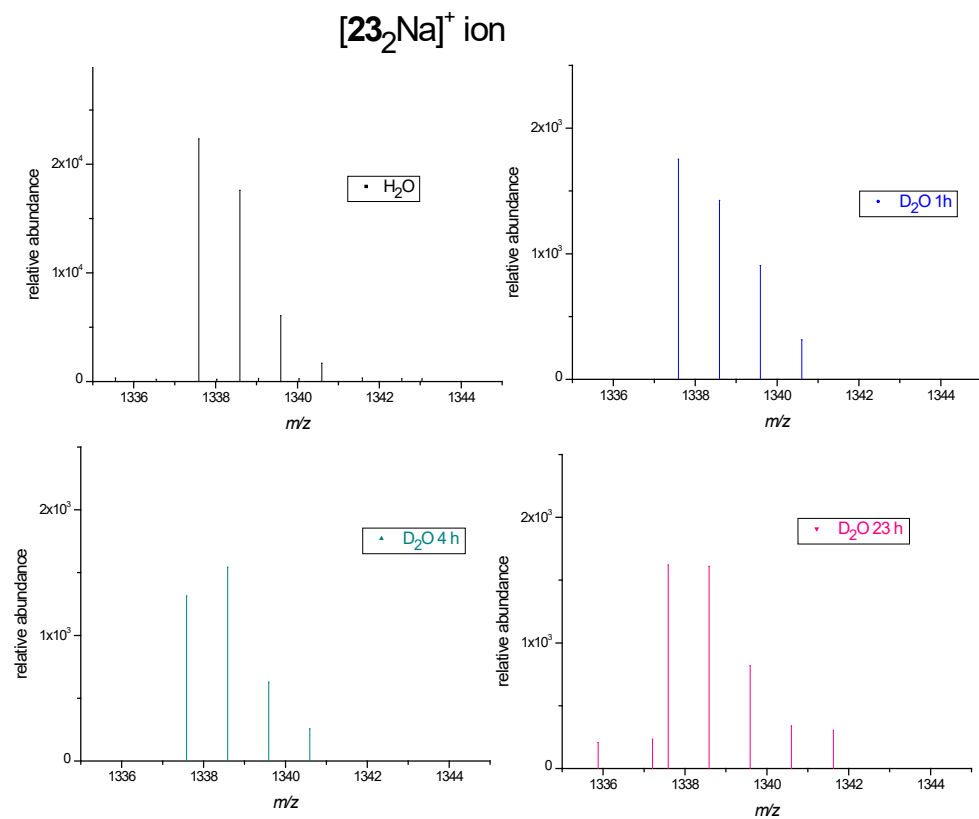


Figure S41 g. Snapshot scan of compound **23** (signal at m/z 1337 assigned as $[23_2+Na]^+$ ion) dissolved in H_2O or D_2O about $10^{-5}M$. The observed signals correspond to the H/D exchange results observed for the single charged dimer ion (sodium adduct) of compound **23**.



3. Computational analysis of 19, 22 and 23

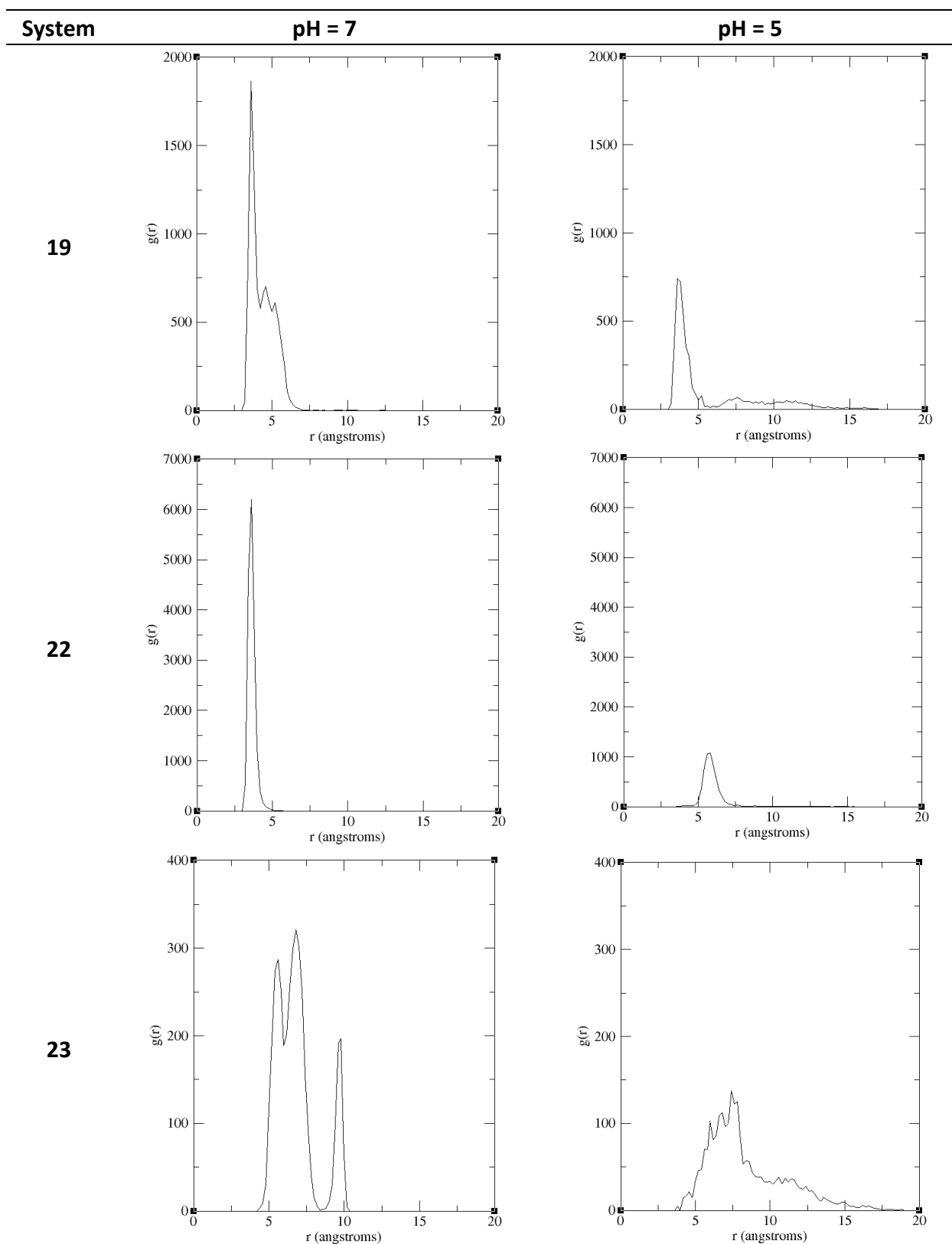


Figure S42. RDF graphs describing the distance between centres of mass of phenanthridine and pyrrole rings during the last 30 ns of the matching molecular dynamics simulations.

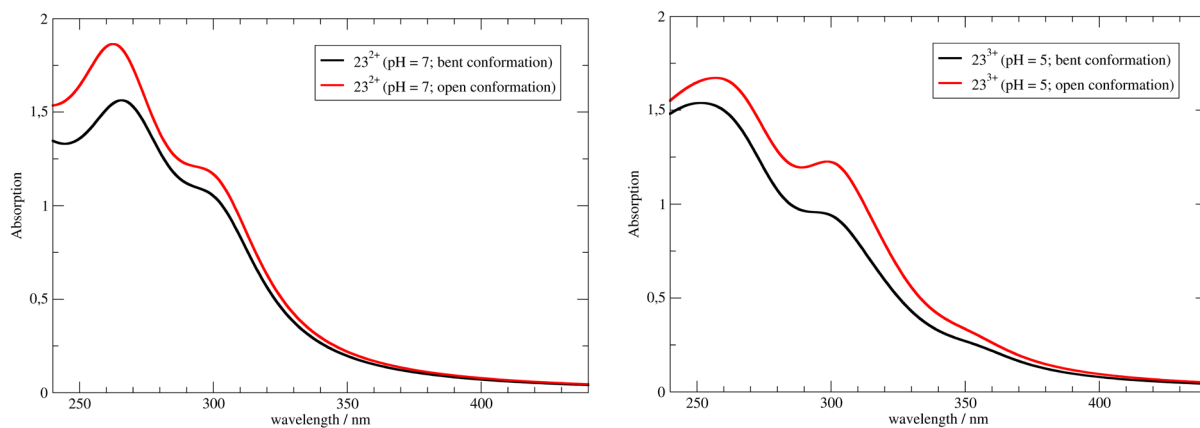


Figure S43. Calculated UV/Vis spectra for the representative structures of both bent and open conformations of systems **23** under normal (pH = 7, left) and acidic conditions (pH = 5, right) obtained with the TD-DFT approach and the (SMD)/B3LYP/6-31+G(d) model in water.